

# The nature of Cu bonding to natural organic matter

Alain Manceau\*, Anthony Matynia

*Mineralogy & Environments Group, LGCA, Université Joseph Fourier and CNRS, 38041 Grenoble Cedex 9, France*

Received 8 September 2009; accepted in revised form 26 January 2010; available online 6 March 2010

## Abstract

Copper biogeochemistry is largely controlled by its bonding to natural organic matter (NOM) for reasons not well understood. Using XANES and EXAFS spectroscopy, along with supporting thermodynamic equilibrium calculations and structural and steric considerations, we show evidence at pH 4.5 and 5.5 for a five-membered Cu(malate)<sub>2</sub>-like ring chelate at 100–300 ppm Cu concentration, and a six-membered Cu(malonate)<sub>1–2</sub>-like ring chelate at higher concentration. A “structure fingerprint” is defined for the 5.0–7.0 Å<sup>-1</sup> EXAFS region which is indicative of the ring size and number (i.e., mono- vs. bis-chelate), and the distance and bonding of axial oxygens (O<sub>ax</sub>) perpendicular to the chelate plane formed by the four equatorial oxygens (O<sub>eq</sub>) at 1.94 Å. The stronger malate-type chelate is a C<sub>4</sub> dicarboxylate, and the weaker malonate-type chelate a C<sub>3</sub> dicarboxylate. The malate-type chelate owes its superior binding strength to an –OH for –H substitution on the α carbon, thus offering additional binding possibilities. The two new model structures are consistent with the majority of carboxyl groups being clustered and α-OH substitutions common in NOM, as shown by recent infrared and NMR studies. The high affinity of NOM for Cu(II) is explained by the abundance and geometrical fit of the two types of structures to the size of the equatorial plane of Cu(II). The weaker binding abilities of functionalized aromatic rings also is explained, as malate-type and malonate-type structures are present only on aliphatic chains. For example, salicylate is a monocarboxylate which forms an unfavorable six-membered chelate, because the OH substitution is in the β position. Similarly, phthalate is a dicarboxylate forming a highly strained seven-membered chelate.

Five-membered Cu(II) chelates can be anchored by a thiol α-SH substituent instead of an alcohol α-OH, as in thio-carboxylic acids. This type of chelate is seldom present in NOM, but forms rapidly when Cu(II) is photoreduced to Cu(I) at room temperature under the X-ray beam. When the sample is wet, exposure to the beam can reduce Cu(II) to Cu(0). Chelates with an α-amino substituent were not detected, suggesting that malate-like α-OH dicarboxylates are stronger ligands than amino acids at acidic pH, in agreement with the strong electronegativity of the COOH clusters. However, aminocarboxylate Cu(II) chelates may form after saturation of the strongest sites or at circumneutral pH, and could be observed in NOM fractions enriched in proteinaceous material. Overall, our results support the following propositions:

- (1) The most stable Cu–NOM chelates at acidic pH are formed with closely-spaced carboxyl groups and hydroxyl donors in the α-position; oxalate-type ring chelates are not observed.
- (2) Cu(II) bonds the four equatorial oxygens to the heuristic distance of 1.94 ± 0.01 Å, compared to 1.97 Å in water. This shortening increases the ligand field strength, and hence the covalency of the Cu–O<sub>eq</sub> bond and stability of the chelate.
- (3) The chelate is further stabilized by the bonding of axial oxygens with intra- or inter-molecular carboxyl groups.
- (4) Steric hindrances in NOM are the main reason for the absence of Cu–Cu interactions, which otherwise are common in carboxylate coordination complexes.

© 2010 Elsevier Ltd. All rights reserved.

\* Corresponding author.

E-mail address: [Alain.Manceau@obs.ujf-grenoble.fr](mailto:Alain.Manceau@obs.ujf-grenoble.fr) (A. Manceau).

## 1. INTRODUCTION

The biogeochemistry of copper is largely controlled by its interactions with natural organic matter (NOM), not so much because of NOM's abundance and polyfunctional character, as because of its remarkable affinity towards Cu(II) relative to other divalent cations (McLaren et al., 1983; Hering and Morel, 1988; Town and Powell, 1993; Ramos et al., 1994; Benedetti et al., 1996; McBride et al., 1997; Leenheer et al., 1998; Kinniburgh et al., 1999; Kogut and Voelker, 2001; Santos-Echeandia et al., 2008). The strong binding ability of NOM for Cu(II) likely results from the excellent match in size between the cupric ion and one or several ligands. The copper ligands must be well-defined structurally and chemically, and also numerous because NOM has a high sorption capacity and selectivity for Cu(II) over a large concentration range (Gao et al., 1997; Covelo et al., 2004). Since carboxylate moieties comprise the large majority of reactive sites below pH 7 in NOM, and can form a vast number of synthetic coordination complexes with Cu(II) (Melnik et al., 1998a,b, 1999), the strongest bonds are expected to be with carboxyl ligands (Sposito et al., 1979; Boyd et al., 1981). The predominance of oxygen ligands does not exclude other electron donors from being involved in Cu bonding, such as nitrogen as suggested by electron spin resonance (ESR) spectroscopy (Boyd et al., 1983; Senesi and Sposito, 1984; Senesi et al., 1985; Luster et al., 1996). Based on solution chemistry the most likely ligands are dicarboxylate (malonate,  $\log K = 5.04$ ), mixed alcohol-carboxylate (citrate, malate,  $\log K = 3.70$  and  $3.63$ ), and aminocarboxylate (glutamate,  $\log K = 8.32$ ) groups attached to aliphatic chains (Fig. 1, Table 1; Gregor et al., 1989a,b; Town and Powell, 1993; Croué et al., 2003). Aromatic dicarboxylate (phthalate,  $\log K = 3.22$ ), alcohol-carboxylate (salicylate,  $\log K = 2.22$  for pH 5), and furan-carboxylate (furanate,  $\log K = 1.10$ ) ligands are less likely, because they have weaker binding strengths than aliphatic ligands. This interpretation is reinforced by infrared spectroscopy and two-dimensional NMR which showed that carboxylate moieties with  $-\text{COOH}$ ,  $-\text{OH}$ , or  $-\text{OR}$  substituents on the  $\alpha$  carbon from aliphatic chains or alicyclic structures constitute the majority of carboxyl structures, with the salicylate and furan-carboxylate aromatic structures being less reactive (Deshmukh et al., 2007; Hay and Myneni, 2007). Therefore, malonate, citrate/malate, and amino acid structures most likely play the important roles in Cu(II) chelation. Although stability constants can be used to predict the a priori nature of Cu(II)-NOM complexes, they do not provide unequivocal information on the true bonding environment of the metal in natural systems. They are, however, extremely valuable for making educated choices on the relevance of model compounds used in structural studies.

Using XANES and EXAFS spectroscopy, and Cu-glutamate as the best-fit structural analog, Karlsson and Skjellberg (2006) showed that Cu(II) forms a five-membered chelate ring with one amino nitrogen ( $\alpha\text{-NH}_2$ ) or alcohol oxygen ( $\alpha\text{-OH}$ ) and one carboxylate oxygen from an  $\alpha$ -substituted aliphatic carboxylic structure (Fig. 1). Copper is bridged to four O/N ligands (CuL<sub>2</sub> complex) in a square-planar geom-

etry at low metal concentration, and to two (CuL complex) at higher concentration. Today the glutamate-like model is the most detailed, but despite its own merit the topic is far from being exhausted. Here are some remaining open questions, which are addressed in this article:

- Is it possible to distinguish oxygen from nitrogen ligands, at least at low Cu concentration when heterogeneity is minimized?
- What are the limits of the glutamate model? Does it always provide an adequate fit to EXAFS data? Since NOM contains several well-defined types of carboxyl structures with specific protonation constants, the coordination mode of Cu(II) should vary with pH, metal to ligand ratio, and chemical composition of the NOM.
- At medium and high Cu concentration, can the data be modeled by a mixture of discrete ligands, and if so, how many are needed?

Answering these questions rests upon three capabilities (i) to detect small variations of the local structure about Cu atoms up to approximately 4 Å (i.e., second C atomic shell), and over two orders of magnitude in concentration (i.e., Cu/C ratio); (ii) to determine from a large dataset of multicomponent spectra the number of independent patterns (or "principal components", PCs) that represent the number of identifiable Cu binding environments (i.e., species) present in the set of spectra; (iii) to build a spectral database of references of known identity and structure, which includes all distinct binding environments seen by EXAFS and plausibly present in NOM.

We recorded our data at liquid helium (LHe) temperature to enhance the signal from higher atomic shells by reducing the lability of organics, and by using a high-flux spectrometer at the European Synchrotron Radiation Facility (ESRF, Grenoble) equipped with a 30-element Ge detector for the study of highly diluted samples (concentration range 100–6500 mg/kg). The significant number of independent patterns accounting for 98–99% of variance in the dataset was determined with principal component analysis (PCA, also known as abstract factor analysis, Malinowski, 1991; Wasserman et al., 1999; Ressler et al., 2000; Manceau et al., 2002). Here, linear algebra can be used for quantification because the EXAFS response from a multi-species sample is the weighted-superposition of the response of each species present in a sample (Manceau et al., 1996). The PCs obtained from the PCA are not real spectra (i.e., they are *abstract* components), but the single species spectra which make up the multicomponent spectra in the dataset are linear combinations of PCs. Thus, the spectra of all unknown species contained in a sample can be identified from a database by target transformation, provided the unknown is present in the library of reference spectra. Care has been taken to include in the database all plausible Cu(II) species discussed in the literature and to not miss any major species. With such an extensive and representative database, target testing goes beyond the usual fingerprinting approach between known and unknown spectra, because the entire dataset is analyzed at one time in a statistically meaningful way for similarity to a specific structural reference.

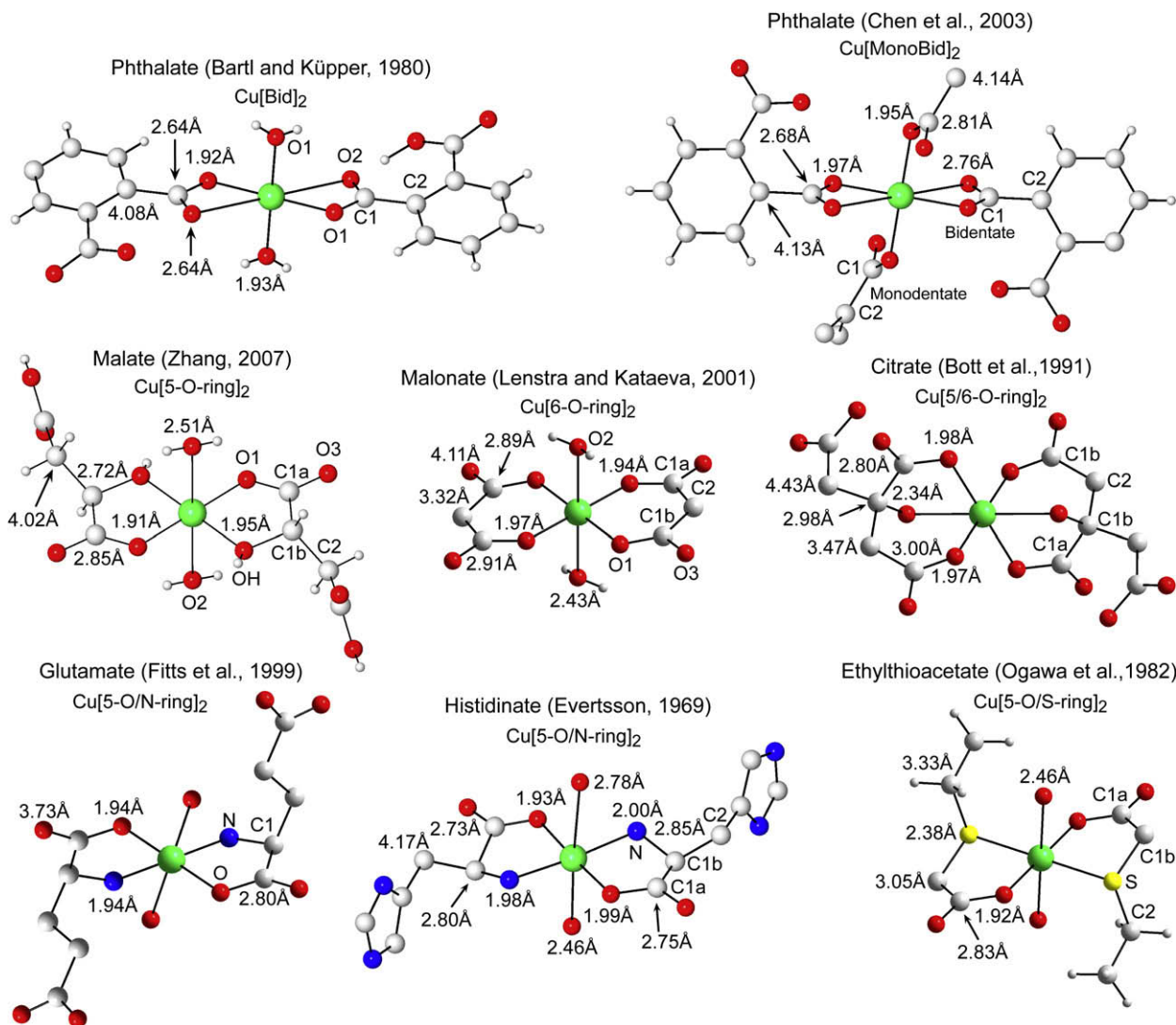


Fig. 1. Structure of Cu organic monodentate and bidentate complexes, and chelates.

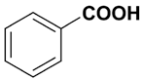
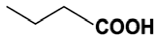
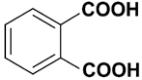
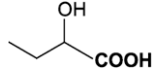
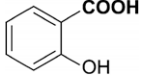
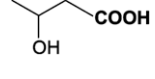
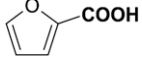
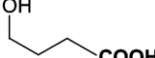
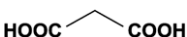
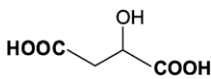
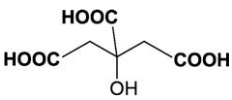
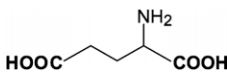
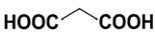
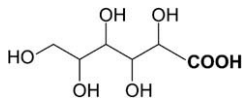
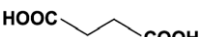
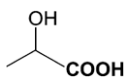
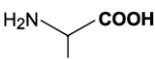
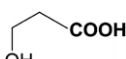
## 2. METHODS

### 2.1. Materials

Copper was sorbed on four types of organic materials considered good representatives of the diversity of NOM: two humic acid standards from the International Humic Substance Society (IHSS #1S102H from the Elliott Soil, and #1S103H from Pahokee Peat in Florida), one peat of heath vegetation (mostly *Carex* sp.) from Mazerolles, northeast of Nantes, France, and one moss peat (mostly *Sphagnum* sp.) from Estonia. The humic acid (HA) and fulvic acid (FA) fractions were extracted from the *Carex* (CP) and *Sphagnum* (SP) peats following the IHSS protocol (Swift, 1996), and also a fraction called here dissolved organic matter (DOM) using the method described by Karlsson and Skjellberg (2006). Organic carbon and nitrogen from the CP and SP samples were measured by combustion with an elemental analyzer (Per-

kin-Elmer, 2400 CHN), and total sulfur with a LECO sulfur analyzer (LECO Corp., MI) (Table 2). The ash fraction was determined by ignition at 900 °C for 5 h. It amounts to 1.5% w/w in SP, and as much as 34.5% w/w in CP, which is a typical value for a nutrient-rich peatland (Bohlin et al., 1989; Ringqvist and Oborn, 2002; Tan, 2003). The elemental composition of CP is reported on an ash-free basis. Mineral matter was eliminated almost completely during fractionation, except for CPDOM which contained some residual inorganic colloids. Although the elemental composition and chemical properties of peat humic substances are believed to be similar to those of humic acids in mineral soils (Mathur and Farnharn, 1985), *Carex* peat has higher nitrogen and sulphur concentrations, while *Sphagnum* peat contains a higher amount of uronic acid, which may modify the binding of Cu (Bohlin et al., 1989). More details on the extraction procedures and physico-chemical characterizations, including <sup>13</sup>C NMR data, can be found in Matynia (2009).

Table 1  
Stability constants of CuL complexes with carboxylate organic molecules ( $I = 0.1$  M; Smith and Martell, 2004).

Compound	Structure	Log <sub>10</sub> <i>K</i>	Compound	Structure	Log <sub>10</sub> <i>K</i>
Benzoate		1.60	Butanoate		1.70
Phthalate		3.22	2-Hydroxybutanoate (α-OH)		2.66 <sup>a</sup>
Salicylate		2.22	3-Hydroxybutanoate (β-OH)		1.82 <sup>a</sup>
Furanate		1.10	4-Hydroxybutanoate (γ-OH)		1.52 <sup>a</sup>
Oxalate		4.85	Malate		3.63
Citrate		3.70	Glutamate		8.32
Malonate		5.04	Gluconate		2.51
Succinate		2.70	Lactate (α-OH)		2.59 <sup>a</sup>
Alanine		8.11	Lactate (β-OH)		1.83 <sup>a</sup>

<sup>a</sup>  $I = 2.0$  M. Catechol is not considered as a likely ligand because it has no carboxyl and two phenolic hydroxyls, which are unreactive at acidic and neutral pH ( $pK_a = 9.3$  and  $13.3$ ). To calculate the amount of CuL in solution at a given pH, one needs to take into account the proton dissociation constant of each functional group. Therefore, the stability constants in the Table reflect the binding strength of the ligand, not its actual capacity to complex Cu at a given pH.

## 2.2. Cu sorption experiments

Uptake experiments were conducted at  $25.0 \pm 0.1$  °C and pH 4.5 or 5.5 in a closed vessel under argon positive pressure. A mass of 0.2 g freeze-dried NOM was suspended in 500 mL of NaNO<sub>3</sub> (Sigma–Aldrich) at  $I = 0.1$  M. The pH values were measured with a combination electrode (Metrohm), and maintained at the desired pH by computer-controlled (718 Stat Titrino, Metrohm) addition of

0.1 M NaOH (Fixanal, Sigma–Aldrich) at  $I = 0.1$  M. For each uptake experiment, a known volume of  $10^{-3}$  M to  $10^{-2}$  M Cu(NO<sub>3</sub>)<sub>2</sub>·3H<sub>2</sub>O was added to the suspension to obtain the desired Cu/C ratio. All suspensions were undersaturated with respect to Cu(OH)<sub>2(s)</sub>. The exact ratio was measured subsequently on dried powder by inductively coupled plasma optical emission spectrometry (Table 2). Twenty-three samples were prepared with Cu concentrations from 100 to 6500 mg/kg dry weight.

Table 2  
Samples names and chemical compositions.

Samples	[Org-C] (g/kg)	[S] (g/kg)	[N] (g/kg)	[Cu] (mg/kg)	[Cu/C] × 10 <sup>3</sup> (mol/mol)
SP10	480	6.2	9.4	100	0.04
SP13 <sup>a</sup>	480	6.2	9.4	130	0.05
SP110	480	6.2	9.4	1100	0.43
SP290	480	6.2	9.4	2900	1.14
SP300 <sup>a</sup>	480	6.2	9.4	3000	1.18
SPHA20	507	6.3	17.0	200	0.07
SPHA20_RT	507	6.3	17.0	200	0.07
SPHA30 <sup>a</sup>	507	6.3	17.0	300	0.11
SPHA260 <sup>a</sup>	507	6.3	17.0	2600	0.97
SPHA470	507	6.3	17.0	4700	1.75
SPHA470_RT	507	6.3	17.0	4700	1.75
SPFA30	486	4.8	42.1	300	0.12
SPFA310 <sup>a</sup>	486	4.8	42.1	3100	1.20
SPFA650	486	4.8	42.1	6500	2.52
SPDOM10	436	11.3	25.0	100	0.04
SPDOM10_RT	436	11.3	25.0	100	0.04
SPDOM30	436	11.3	25.0	300	0.13
SPDOM30_RT	436	11.3	25.0	300	0.13
CP32	472	17.8	21.8	320	0.13
CP230	472	17.8	21.8	2300	0.92
CPHA20	446	13.7	28.6	200	0.08
CPHA160	446	13.7	28.6	1600	0.68
CPFA34	456	6.4	10.1	340	0.14
CPFA490	456	6.4	10.1	4900	2.03
CPDOM30	296 <sup>b</sup>	15.0	20.0	300	0.19
ESHA200 <sup>c</sup>	–	–	–	2000	–
FPHA200 <sup>c</sup>	–	–	–	2000	–

<sup>a</sup> Sorption samples prepared at pH 5.5. All others were prepared at pH 4.5. All EXAFS spectra were recorded at 10 K, except those labelled with the RT extension.

<sup>b</sup> This fraction contains inorganic colloids.

<sup>c</sup> Elliott Soil (ES) and Florida (Pahokee) peat HA from the IHSS.

### 2.3. Cu coordination complexes

Five crystalline organometallic complexes of known structure were synthesized and their purity verified by X-ray diffraction. The binding environment of Cu in each of them is shown in Fig. 1.

- Cu(II) bis(hydrogen *o*-phthalate)dihydrate ( $\alpha$ -Cu(C<sub>8</sub>H<sub>5</sub>O<sub>4</sub>)<sub>2</sub>·2H<sub>2</sub>O; Cingi et al., 1969; Bartl and Küppers, 1980; Goeta et al., 1993), a bis-bidentate complex denoted Cu[Bid]<sub>2</sub>.
- Cu(II) bis(hydrogen *o*-phthalate)dinitrate dihydrate (Cu(C<sub>16</sub>H<sub>8</sub>O<sub>8</sub>)Na<sub>2</sub>·2H<sub>2</sub>O; Chen et al., 2003), a bis-mono-dentate–bidentate complex denoted Cu[MonoBid]<sub>2</sub>.
- Cu(II) di(hydrogen malonate) dihydrate (Cu(C<sub>6</sub>H<sub>10</sub>O<sub>10</sub>), Cu(malonate)<sub>2</sub>; Lenstra and Kataeva, 2001), a bis-six-membered carboxyl chelate denoted Cu[6-O-ring]<sub>2</sub>.
- bis-L-histidinecopper(II) dinitrate dihydrate (Cu(C<sub>6</sub>H<sub>9</sub>O<sub>2</sub>N<sub>3</sub>)<sub>2</sub>·2(NO<sub>3</sub>,H<sub>2</sub>O); Evertsson, 1969), a bis-five-membered amino acid chelate denoted Cu[5-O/N-ring]<sub>2</sub>.
- Cu(II) gluconate (Cu(C<sub>6</sub>H<sub>10</sub>O<sub>7</sub>)(C<sub>10</sub>H<sub>9</sub>N<sub>3</sub>)(H<sub>2</sub>O)·3(H<sub>2</sub>O); Yodoshi et al., 2006), a Cu[5/6-O/N-ring]<sub>2</sub> chelate.

This series was completed with five aqueous complexes.

- Cu(II) di-malate, a bis-five-membered carboxyl chelate with a Cu bonding environment similar to the solid ana-

log Cu(C<sub>6</sub>H<sub>5</sub>O<sub>5</sub>)<sub>2</sub>(H<sub>2</sub>O)<sub>2</sub> (Zhang, 2007). This chelate is denoted Cu[5-O-ring]<sub>2</sub>.

- Cu(II) di-lactate (Cu(lactate)<sub>2</sub>), a bis-five-membered carboxyl chelate with a Cu bonding environment similar to the solid analog Cu(C<sub>3</sub>H<sub>5</sub>O<sub>3</sub>)<sub>2</sub>·1.5H<sub>2</sub>O (Prout et al., 1968).
- Cu(II) mono and bis-citrate, two five-six-membered carboxyl chelates with a Cu bonding environment similar to the solid analog Cu(C<sub>6</sub>H<sub>5</sub>O<sub>7</sub>)<sub>2</sub>(NH<sub>4</sub>)<sub>4</sub> (Bott et al., 1991)). The two chelates are denoted Cu[5/6-O-ring] and Cu[5/6-O-ring]<sub>2</sub>.
- Cu(II) di-thiolactate, a bis-five-membered sulfhydryl/carboxyl chelate with a Cu bonding environment similar to that in Cu(II) ethylthioacetate (Ogawa et al., 1982). It is denoted Cu[5-O/S-ring]<sub>2</sub>.

### 2.4. Data collection and reduction

The XANES and EXAFS spectra for sorption samples were measured in fluorescence-yield mode on pressed pellets. Measurements were carried out on the FAME beamline (BM 30B; Proux et al., 2006) at the ESRF and liquid helium temperature to prevent sample damage by photoreduction (Powers, 1982; Manceau et al., 2002), except for samples SPHA20, SPHA470, SPDOM10, and SPDOM30



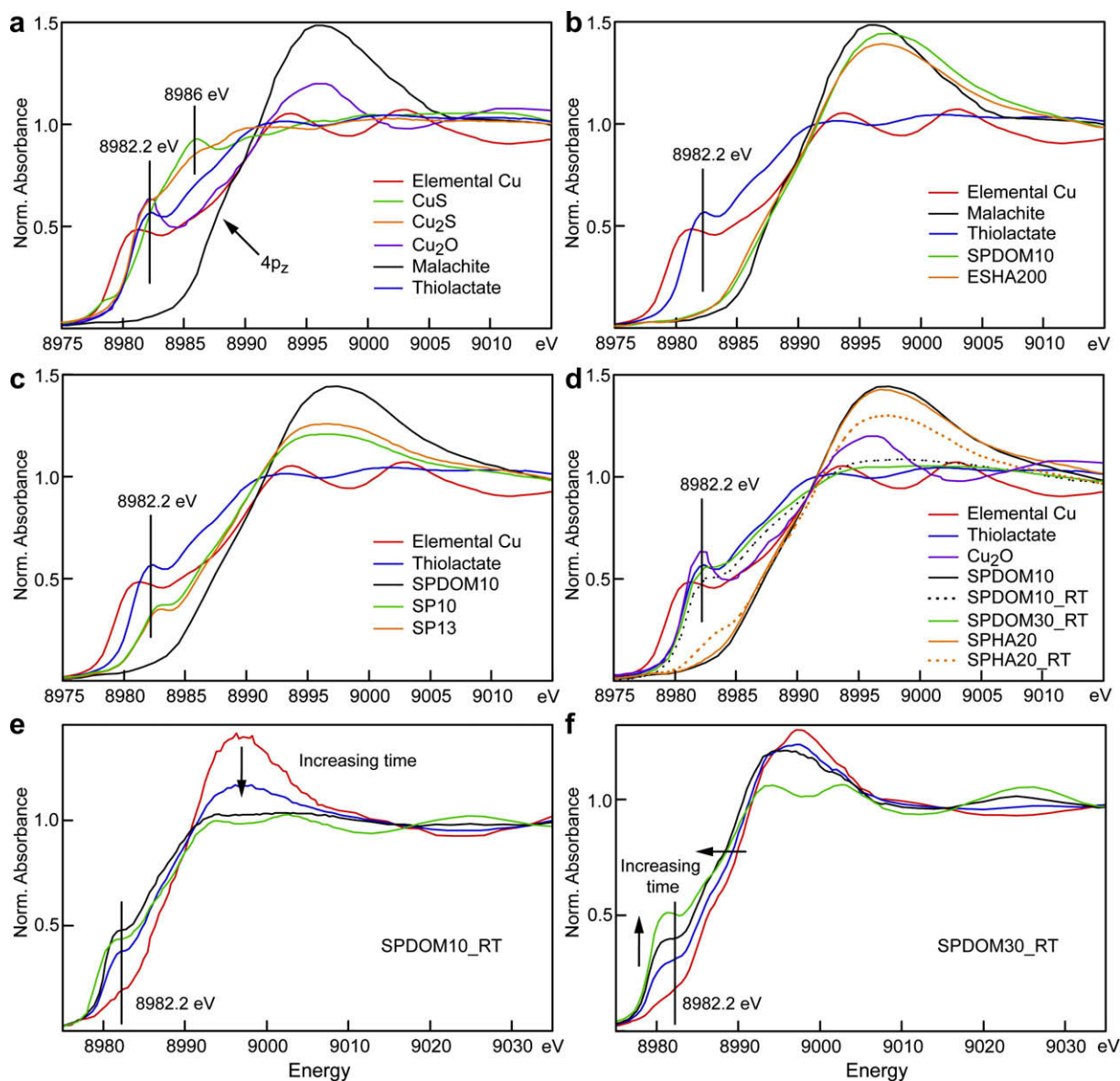


Fig. 2. Normalized Cu K-edge XANES spectra of samples and references.

which were measured at both low and room temperature (RT, Table 2). The XANES spectra of the two DOM fractions from SP (SPDOM10 and SPDOM30) were measured also on the microfocus beamline 10.3.2. (Marcus et al., 2004) of the Advanced Light Source (ALS, Berkeley) at RT. The EXAFS spectra of the crystalline references were collected in transmission mode at RT on 10.3.2, and those for aqueous chelates at RT (Cu(citrate)<sub>1-2</sub>) or liquid helium on frozen solutions (Cu(malate)<sub>2</sub>; Cu(lactate)<sub>2</sub>; Cu(thiolactate)<sub>2</sub>) in fluorescence mode on FAME. The absolute energy of XANES spectra is referenced to the first inflection point of pure Cu at 8979 eV. EXAFS data were analyzed with WinXAS (Ressler, 1998), and simulated with amplitude and phase shifts functions generated by FEFF v.7 (Ankudinov and Rehr, 1997), using acetate dihydrate (Wang et al., 2006) as structure model. The PCA code is described in Manceau et al. (2002).

### 3. RESULTS

#### 3.1. XANES spectroscopy

##### 3.1.1. Cu(II) reference compounds

When Cu is monovalent and coordinated to O (e.g., Cu<sub>2</sub>O), a well-defined absorption feature from the 1s to 4p<sub>x,y</sub> transition occurs at 8982 eV (Kau et al., 1987) (Fig. 2a). This feature is less salient when Cu(I) is coordinated to S (e.g., Cu<sub>2</sub>S), because of the hybridization of Cu-d and S-p states. When S is bonded to Cu(II) (e.g., CuS) instead of Cu(I), it occurs at higher energy (8986 eV), partly because of the chemical shift of the 1s core level of Cu(II) relative to Cu(I). The high degree of covalency of the Cu–S bonds in these two sulfurs produces spectra with similar shapes. Divalent Cu coordinated to six (4 + 2) O/N in tetragonal configuration (Jahn–Teller distortion;

Cotton et al., 1999) gives an intense absorption maximum ('white line') at 8996 eV from the 1s to continuum transition, and two weak features at 8978 eV from the 1s to 3d transition and  $\sim$ 8988 eV from the 1s to 4p<sub>z</sub> transition with a simultaneous ligand–metal charge-transfer shakedown transition (e.g., malachite Cu<sub>2</sub>(OH)<sub>2</sub>CO<sub>3</sub>) (Bair and Goddard, 1980; Hahn et al., 1982; Grunes, 1983; Kosugi et al., 1984). Since the 4p<sub>z</sub> orbital is oriented along the elongation axis of the Cu(II) pseudo-octahedron, this transition can be used to estimate the extent of the tetragonal distortion caused by the Jahn–Teller effect (Frenkel et al., 2000; Dupont et al., 2002). When Cu is bonded to both S and O, as in thiolactate, the covalent Cu–S bond contributes intensity at 8982 eV and at higher energy with an absorbance intermediate between the Cu–S and Cu–O references. All these results are consistent with earlier studies. For a more detailed analysis of Cu XANES spectra in terms of symmetry of the Cu–O and Cu–S bonds, the reader can consult the article by Kau et al. (1987).

### 3.1.2. NOM samples

Except for a few cases, all samples have a XANES spectrum typical of Cu(II) with a six-fold coordination by O/N donors (regardless of their protonation) in a tetragonally-distorted environment, as illustrated in Fig. 2b with SPDOM10 and ESHA200. The splitting of the 4p orbitals is 5.5 eV (Fig. 3), corresponding to an apical Cu–O bond length of about 2.35 Å compared to about 1.95 Å for the equatorial distances (Dupont et al., 2002). A distinctive coordination environment was identified in the SP peat samples SP10 and SP13 (Fig. 2c). Their spectra are characterized by a sharp peak at 8983 eV, an absorbance in the rising part of the edge shifted in the direction of thiolate, and an edge maximum  $\sim$ 0.5 eV below the maximum of the Cu(II)–O complexes. These two spectra look to be composite and could be reproduced with linear combinations of 50% SPDOM10 + 50% thiolactate (SP10) and 55% SPDOM10 + 45% thiolactate (SP13). Sulfur bonds also were detected in the air-dried DOM and HA fractions of the SP peat, but only at low concentration and room

temperature (SPDOM10\_RT, SPDOM30\_RT, and SPHA20\_RT) (Figs. 2d and 3). The proportion of the Cu–S pairs increased with time during measurements at RT, while the spectra for these samples were immune to exposure time at 10 K. Thus, these pairs were not present in the initial samples and formed under the beam at RT beam. Divalent copper has a low standard electrode potential, and thus can be easily reduced in solution to Cu(I) and even elemental Cu by free electrons, radicals, H<sub>2</sub>, and other species derived from the radiolysis of water by ionizing X-rays (Mesu et al., 2006). Here, the Cu–S bonds were probably generated subsequently to the production of Cu(I) because this species has a high thiophilicity similar to that of Hg(II) (Dance, 1986; Wright et al., 1990). The two DOM samples have a higher proportion of Cu–S bonds than SPHA20\_RT, consistent with the higher hygroscopic properties of these small water-soluble humic-like organics, and with the higher amount of sulfur in this fraction (1.13 vs. 0.62 wt.%, Table 2).

To test this hypothesis, the two most easily damaged samples, SPDOM10 and SPDOM30, were analyzed in a moist state at RT using a two-times higher flux density with micro-XANES spectroscopy (Marcus et al., 2004). Under this more intense beam, Cu(II) to Cu(I) reduction in SPDOM10 began after a few minutes of exposure, and the amount of Cu–S bonds increased during the first 2 h of measurement (Fig. 2e). Longer exposure led to the detection of Cu<sup>0</sup>. In SPDOM30, Cu(II) was reduced directly to Cu<sup>0</sup> within minutes, without evidence for intermediate formation of Cu(I) (Fig. 2f). After several scans on the same spot, a small displacement of the sample under the X-ray spot and reexamination showed little reduction, indicating that the effect was limited to the X-ray footprint. SPHA20 was examined also by micro-XANES, but in the dried state. Some Cu(I) formed after  $\sim$ 30 min exposure time, but the kinetics of reduction was much lower than with SPDOM and Cu<sup>0</sup> was never detected. These results show that Cu(II) bound to organics does not survive under high-flux conditions, the reduction rate and nature of the end-product are variable and related, among other factors, to exposure time, sample humidity, Cu/S ratio, and total Cu. In a study on the binding of Cu(II) to aquatic humic substances, Frenkel et al. (2000) observed at low Cu/C ratio an intriguing feature at about 8979 eV, which they assigned to Cu–N bonds. The same feature was reported by Karlsson and Skyllberg (2006) on low-Cu DOM prepared as wet paste, also providing suggestive evidence for the involvement of N-containing functional groups in the first coordination shell of Cu(II). From our results, this feature is most likely an adverse effect.

## 3.2. EXAFS spectroscopy

### 3.2.1. Cu(II) reference compounds

Copper(II) carboxylates form a large and structurally diverse class of compounds comprising monomeric, dimeric, and polymeric structures, with occasional amine nitrogen and thiolate sulfur ligands in addition to the predominant carboxyl ligands (Melnik et al., 1998a,b, 1999). In addition, carboxyl anions can act as monodentate and bidentate li-

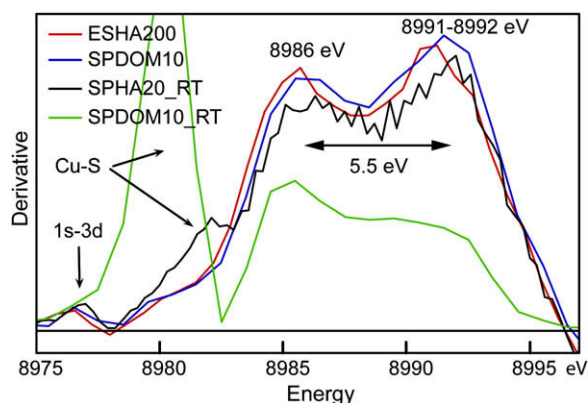


Fig. 3. Derivative of XANES spectra showing the splitting of the 4p orbitals resulting from the Jahn–Teller distortion (ESHA200, SPDOM10), and the formation of Cu–S bonds at room temperature (SPHA20\_RT, SPDOM10\_RT).

gands, and participate in five-, six- or higher membered ring chelates (Fig. 1). For steric reasons, the first C shell (C1) is closest to Cu in a bidentate complex (Cu[Bid]). From the survey of crystallographic data, the C1 shell is at 2.6–2.7 Å in this complex, and 2.7 to ~3.3 Å in monodentate complexes (Cu[Mono]) and ring chelates (Fig. 4, Table EA1). In five-membered rings (Cu[5-O-ring]), the C1 shell contains two atoms at the split distance of 2.7–2.8 Å (C1a) and 2.8–2.9 Å (C1b), except in the highly symmetrical  $\beta$ -CuC<sub>2</sub>O<sub>4</sub>·0.4H<sub>2</sub>O oxalate chelate where the two C atoms are at 2.70 Å. In six-membered rings (Cu[6-O-ring]), the C1a and C1b atoms are at 2.8–3.0 Å, and the third ring-forming C atom (C2) forms a distinct shell at 3.2–3.3 Å. This Cu–C distance is diagnostic of Cu[6-O-ring], because the second C shell is at ~4.1 Å in Cu[Bid] and 3.7–5.0 Å in Cu[Mono]. Therefore, monodentate, bidentate, and five- and six-membered coordination modes can be identified by EXAFS from the distances of the C1 and C2 shells. Seven-ring chelates have been described in only two phthalates (Table EA1). These compounds have Cu–C2 distances similar to Cu[Mono] complexes, because the Cu atoms are attached also monodentally to other carboxyl groups from adjacent phthalate groups. Practically, Cu coordination complexes can be discerned by comparing the magnitude and imaginary parts of the Fourier transform (FT) from the EXAFS signal in the [1.9–3.0 Å]  $R + \Delta R$  interval ( $\Delta R \sim -0.4$  Å to  $-0.5$  Å), as illustrated in Fig. 5 with seven model compounds.

The >0.1 Å separation of the C1 distances in bidentate and monodentate/five-ring structures is shown in Fig. 5a with the FTs of the Cu[Bid]<sub>2</sub> and Cu[5-O-ring]<sub>2</sub> references. When these two coordinations coexist in the same structure, as in Cu[MonoBid]<sub>2</sub>, then the second FT peak is a doublet, and its imaginary part and EXAFS spectrum are intermediate between those of Cu[Bid]<sub>2</sub> and Cu[5-O-ring]<sub>2</sub> (Fig. 5b). Cu[6-O-ring]<sub>2</sub> has a peak at 2.8 Å  $R + \Delta R$ , which is the signature of the C2 shell at  $R \sim 3.32$  Å (Fig. 5c). Citrate ion is a tridentate ligand, which acts as a 5-membered and 6-membered chelate by bridging Cu through two carboxyl O and one  $\alpha$ -OH. This configuration is characterized by an intense second peak and a C2 shell at 3.47 Å (Fig. 5d). Divalent copper also forms stable five-membered heterocyclic chelates with N/O and S/O coordinating ligands, as in proteins (Gazo et al., 1976; Ogawa et al., 1982). Here, histidine was used as a representative of Cu(II) binding to amino N and carboxyl COOH groups. Since the Cu–N distance is on average slightly longer (~2.00 Å) than the Cu–O distance (~1.95–1.96 Å) (Freeman et al., 1964; Orpen et al., 1994), the EXAFS frequency for this chelate is shifted to the left and the position of the first FT peak to the right relative to Cu[5-O-ring]<sub>2</sub> (arrows in Fig. 5e). However, detecting Cu–N bonds in the presence of Cu–O interactions is generally difficult, because O and N have similar sizes and phase and amplitude functions in EXAFS (D'angelo et al., 1998; Carrera et al., 2004). It is possible in histidine because the EXAFS spectrum is from a single bonding environment, but NOM has multiple binding configurations with a predominance of O ligands, at least at intermediate and high Cu concentration, which makes Cu–N bonds

undetectable. When Cu is bonded to both O and S atoms, the shift in frequency of the EXAFS signal and position of the first FT peak is much higher, by virtue of the larger size of S and its stronger scattering properties (Fig. 5f). This coordination fingerprint can be illustrated with thiolactate, a thiolate–carboxylate bifunctional ligand like L-cysteine in proteins (Briand et al., 2004). Similarly to  $\alpha$ -OH and  $\alpha$ -NH<sub>2</sub> substituted carboxylates, thiolactate is a five-membered heterocycle imposed by the  $\alpha$ -SH substitution (Fig. 1).

Thus, the FTs exhibit shapes in the [1.9–3.0 Å]  $R + \Delta R$  interval characteristic of the type, number and arrangement of atoms in the first three shells around Cu(II) in carboxylates, providing “structural fingerprints” that are unique to specific coordinations. This occurs because the EXAFS spectrum is dominated in this interval by single scattering (SS) events, allowing deduction of  $R + \Delta R$  distances of the O/N, C, and S shells directly from peak positions. Three-body Cu–O1–C1 multiple scattering (MS) contributions with effective path lengths of 3.1–3.4 Å are negligible because the scattering angle is always less than 160° (D'Angelo et al., 1998). The other significant paths, such as O1–Cu–O1 in all planar complexes and Cu–C1–O3 in five-membered chelates, have a path length of ~3.9 Å, thus producing a FT peak at 4.4 Å  $R + \Delta R$  outside the fingerprint window. The three-body contributions from monodentate, bidentate (Cu–C1–C2), and six-membered (Cu–C1–O3) structures have even longer path lengths, which appear to be too long to give distinctive peaks on FTs.

### 3.2.2. Cu bonding in NOM

#### 3.2.2.1. Number of identifiable structural configurations.

Since NOM is a polyfunctional complexant, Cu likely is bonded to more than one functional group in proportions that may vary with the metal concentration, the pH, and the chemical composition of the organic matter, which is a function of its origin and how it was extracted from the source material. Thus, any EXAFS spectrum of NOM is a weighted average of all Cu bonding environments present, which may differ from sample to sample. The number of Cu–NOM complexes identifiable by EXAFS spectroscopy in the sample series we investigated was evaluated by PCA using three criteria:

- The amplitude of each component weighted by eigenvalues, which is directly related to how much of the signal the PC represents (i.e., % of the variance).
- The variation of the fit total (normalized total squared residual, NSS-Tot), which was obtained by successively including additional components in the reconstruction of the dataset.
- The indicator value (IND parameter) of each component, which is supposed to reach a minimum for the least significant component.

The PCA was performed in the [2.0–11.6 Å<sup>-1</sup>]  $k$  interval on the complete set of EXAFS spectra from Cu-complexed NOM collected at both helium and room temperature (27 in total). The output parameters, including eigenvalues, the variance, IND, NSS-Tot, and the marginal variation of



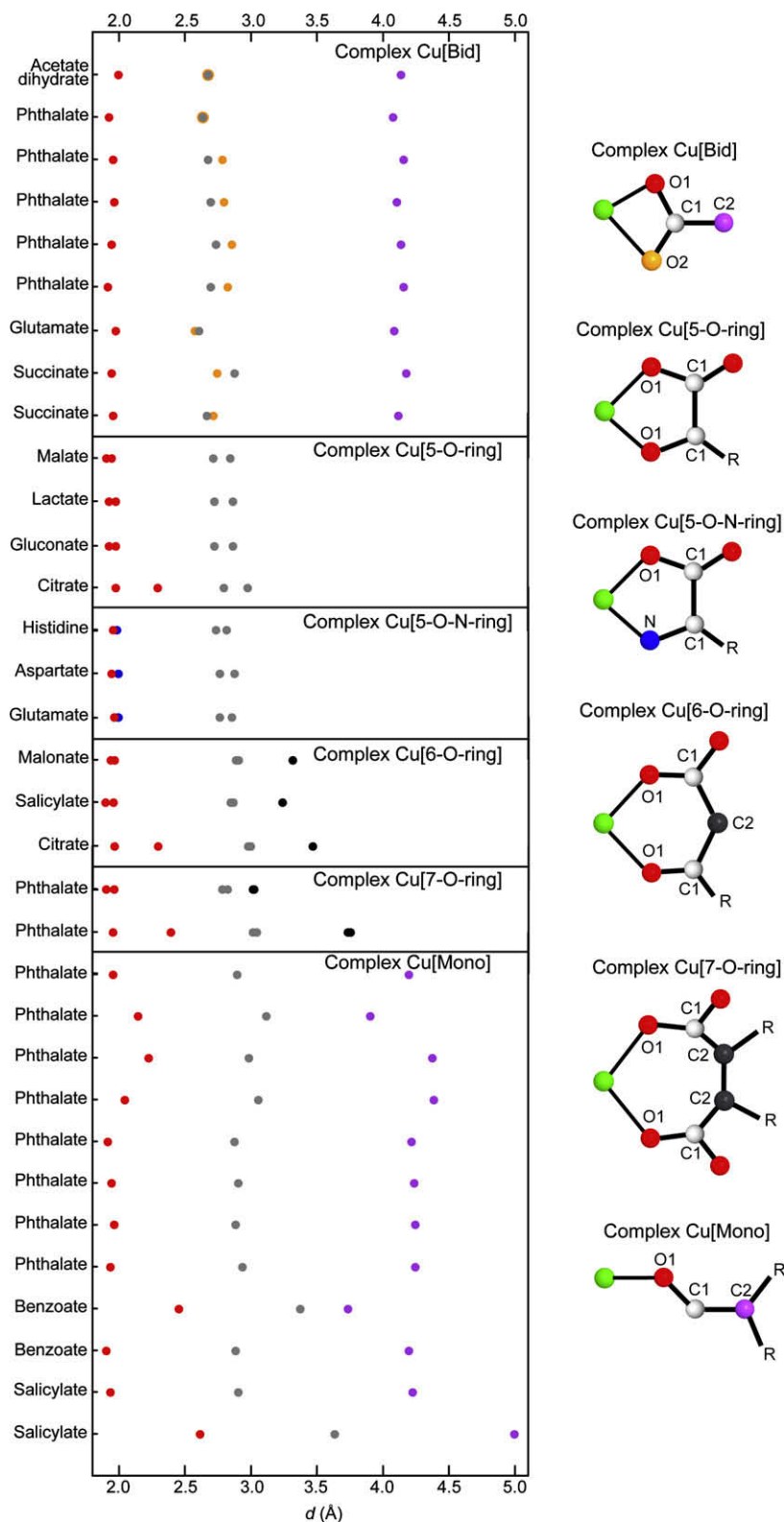


Fig. 4. Relationship between Cu(II)-(O,C) distances and Cu(II) bonding environment in coordination complexes. See Table EA1 for details.

NSS-Tot when a new component is added, are given in Table 3 for the six most significant principal components. The component spectra (i.e., the orthonormal eigenvectors) are

shown in Fig. 6, and the best linear reconstruction of all sample spectra with the two main components (PCs) in Fig. EA1. From visual inspection of all PCs, only the first

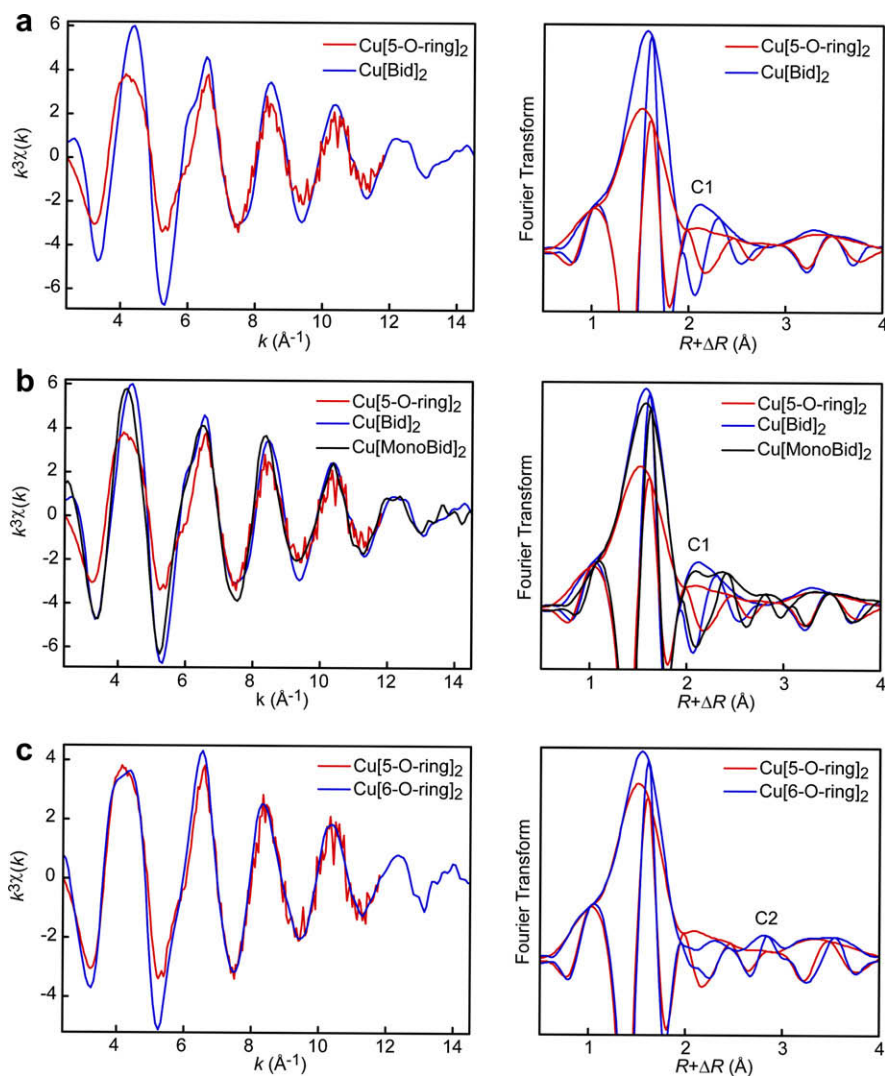


Fig. 5. EXAFS spectra and Fourier transforms (FTs) of model compounds. Cu[Bid]<sub>2</sub> = bidentate complex with phthalate (powder, RT); Cu[MonoBid]<sub>2</sub> = monodentate and bidentate complex with phthalate (powder, RT); Cu[5-O-ring]<sub>2</sub> = five-membered chelate with malate (solution frozen at 10 K); Cu[5-O/N-ring]<sub>2</sub> = five-membered chelate with histidine (powder, RT); Cu[6-O-ring]<sub>2</sub> = six-membered chelate with malonate (powder, RT); Cu[5/6-O-ring]<sub>2</sub> = five- and six-membered chelate with citrate (2:1 complex, solution at RT); Cu[5-O/S-ring]<sub>2</sub> = five-membered chelate with thiolactate (binding environment analog to ethylthioacetate; 2:1 complex, solution frozen at 10 K). The FTs are uncorrected for phase shift, resulting in FT distances approximately 0.4 Å shorter than the actual interatomic distances reported in Table EA2.

two, and perhaps the third, have sufficient weight to look like real EXAFS spectra. The first two PCs account for  $94 + 4 = 98\%$  of the variance in the data, and deviations between data and reconstructions based on two components were small with normalized sum-squared (NSS) values from 0.01 to 0.081, and a NSS-Tot of 0.038. Inclusion of PC#2 to the one-component fit reduced NSS-Tot by 52 %, inclusion of PC#3 improved the two-component fit by 26 %, and inclusion of PCs #4, 5 and 6 successively in series improved the fit by a smaller and similar margin (12–14%, Table 3), indicating statistical noise only. Also, the decline of the eigenvalues from the PCA, which rank PCs according to their importance in reproducing a dataset, is discontinuous, decreasing steadily from the

first to the second, and second to the third, component, and slowly afterwards reaching a quasi-plateau. The IND parameter also suggests three PCs, but this indicator is less reliable than the marginal decline of the eigenvalues and variance with the number of PCs (Manceau et al., 2002; Sarret et al., 2004; Panfili et al., 2005; Kirpichtchikova et al., 2006). In summary, the 27 sample spectra can be reconstructed within error with only three independent components, two being major and one minor, suggesting that all NOM samples can be described quantitatively by variable amounts of essentially two to three well-defined and distinct bonding environments. The three generic configurations of Cu bonding to NOM are identified next by target transformation.

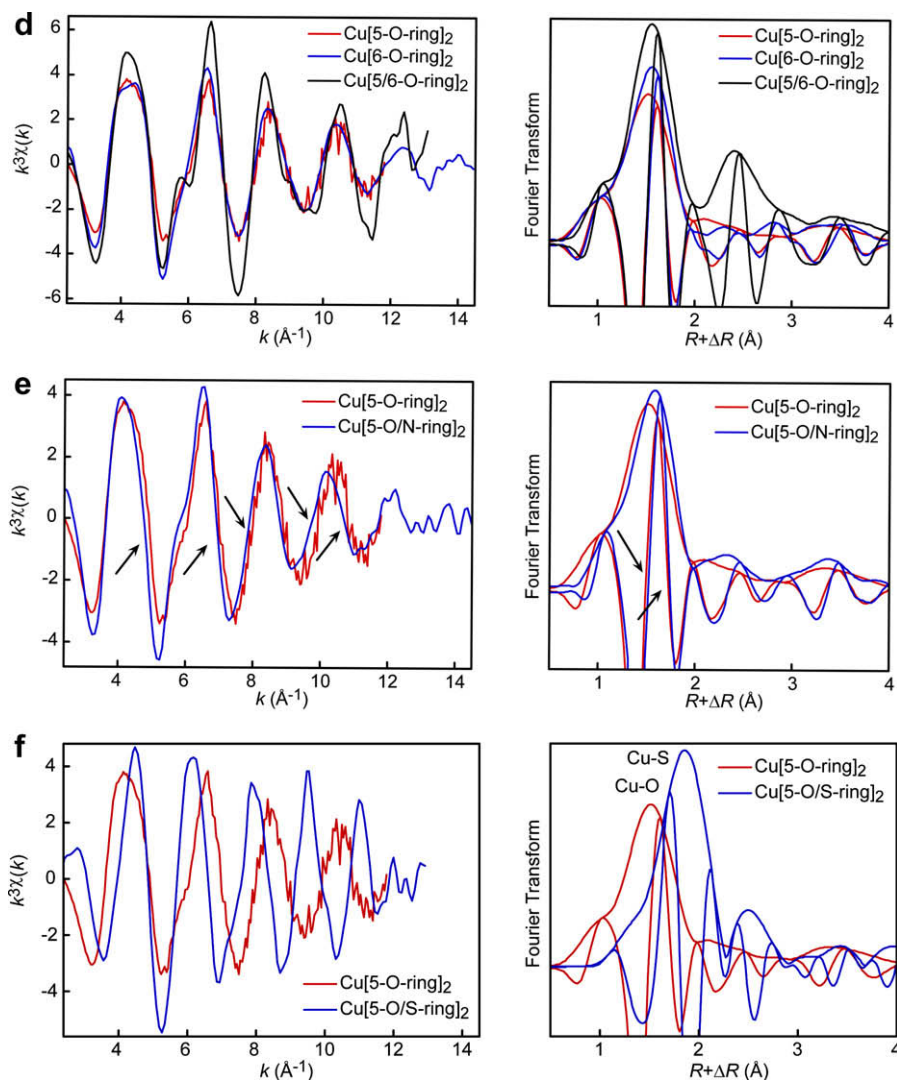


Fig. 5 (continued)

Table 3  
Results from the PCA in the  $[2.0\text{--}11.6 \text{ \AA}^{-1}]$   $k$  interval.

PC# <sup>a</sup>	Eigenvalue <sup>b</sup>	% of variance <sup>c</sup>	IND $\times 10^{3d}$	NSS-Tot $\times 10^{2e}$	% of variation <sup>f</sup>
1	149	94	12.7	7.9	–
2	31.5	4	9.7	3.8	52
3	15.8	1	9.2	2.8	26
4	9.4	0.4	9.5	2.4	14
5	9.0	0.3	9.9	2.1	12
6	7.9	0.2	10.4	1.8	14

<sup>a</sup> Principal component number ( $i$ ).

<sup>b</sup> Values of the diagonal matrix in the PCA after consecutive elimination of the components. Eigenvalues rank PCs according to their importance to reproduce data.

<sup>c</sup> Calculated from the first 6th components.

<sup>d</sup> Malinowski (1977) indicator value.

<sup>e</sup> Normalized sum-squared total =  $\sum_{\text{spectra}} \sum_n [k^3\chi(k_n)_{\text{exp}} - k^3\chi(k_n)_{\text{reconst}}]^2 / \sum_{\text{spectra}} \sum_n [k^3\chi(k_n)_{\text{exp}}]^2$ . This parameter is the normalized sum-squared (NSS) residual of the entire set of data, taken as one.

<sup>f</sup> Marginal variation of NNS-Tot =  $[(\text{NSS-Tot})_i - (\text{NSS-Tot})_{i+1}] / (\text{NSS-Tot})_i$ .

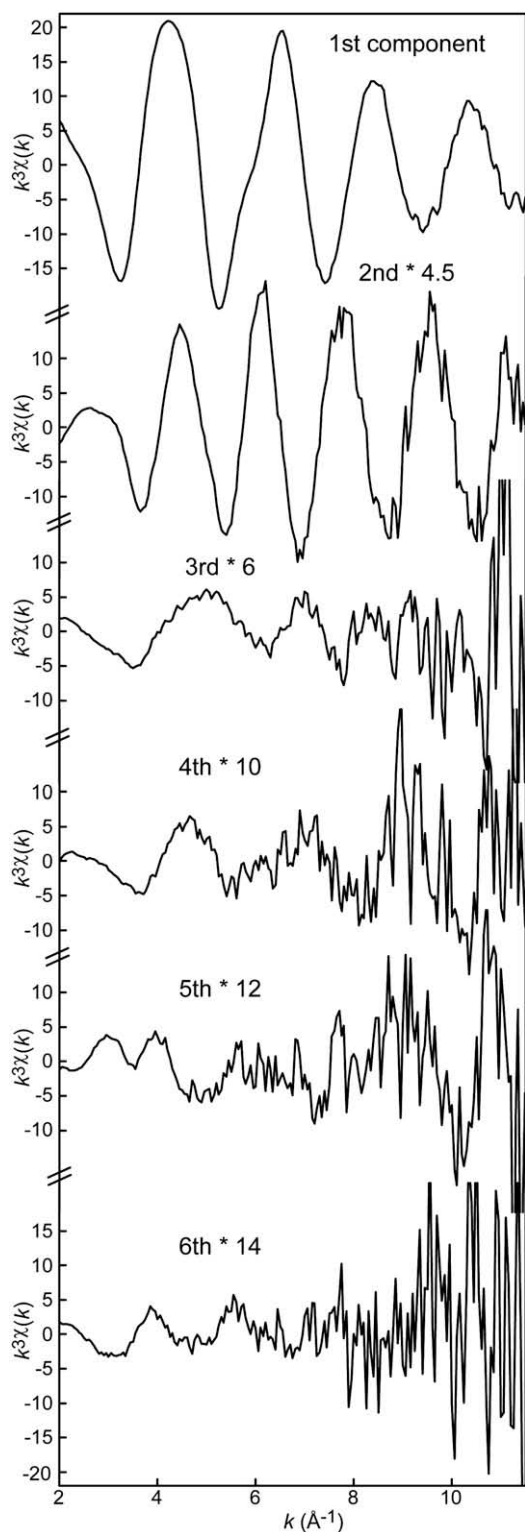


Fig. 6. First six principal components weighted by eigenvalues ( $\lambda$ ) of the  $k^3\chi(k)$  spectra for the 27 spectra presented in Fig. EA1. For clarity, the amplitudes of the 2nd, 3rd, 4th, 5th, and 6th components have been multiplied by 4.5, 6, 10, 12, and 14, respectively.

**3.2.2.2. Types of structural configurations.** In target transformation, a reference spectrum is tested by removing from it all signal not describable as a linear combination of the

PCs (Manceau et al., 2002). The degree to which the target-transformed candidate truly resembles the original reference spectrum is given by the SPOIL value. A high SPOIL means that the reference cannot be described as a sum of the PCs and is therefore not a likely component of the dataset. Usually, references with SPOIL values  $<1.5$  are considered excellent, 1.5–3 good, 3–4.5 fair, 4.5–6 poor and  $>6$  unacceptable (Malinowski, 1978). However, these limits are indicative only because the SPOIL value of a spectrum depends on the  $k$  interval of the calculation. In contrast to the sum-squared residual, SPOIL increases when  $k_{\max}$  is diminished, which is counterintuitive. In fact the SPOIL parameter is more complicated than just a sum-squared. The parameter takes into account such things as the number of degrees of freedom, which changes with the size of the dataset, and the failure of the reconstruction, which is easier to detect at low  $k$  where the residual is smooth and nearly noiseless (Fig. 7). To obtain a sense of how SPOIL varies with  $k_{\max}$ , its value was calculated in the extended  $[2.0\text{--}11.6 \text{ \AA}^{-1}]$  and reduced  $[2.0\text{--}10.0 \text{ \AA}^{-1}]$   $k$  intervals for the seven most relevant references described previously and for CuS and oxalate. None of them fell into the excellent category, but two were good to fair: thiolactate ( $\text{Cu}[5\text{-O/S-ring}]_2$ , 1.9–2.3) and malonate ( $\text{Cu}[6\text{-O-ring}]_2$ , 2.9–4.2). Histidine ( $\text{Cu}[5\text{-O/N-ring}]_2$ , 4.2–5.7) and malate ( $\text{Cu}[5\text{-O-ring}]_2$ , 4.5–5.6) ranked just behind, suggesting the occurrence of some five-ring chelates. This interpretation is consistent with the fifth score obtained by citrate (5.1–6.0), because the two different sizes of ring chelates coexist in this molecule (Fig. 1). Bidentate complexation ( $\text{Cu}[\text{Bid}]_2$ ) is unlikely (7.5–11.3), but the same Cu atom may be both monodentally and bidentally coordinated to two separate ligands ( $\text{Cu}[\text{MonoBid}]_2$ , 5.8–7.8). With SPOIL values of 13.0–16.5 and 14.7–18.5, CuS and oxalate are clearly not good structural models for the complexation of Cu in NOM.

**3.2.2.3. Six-O-ring chelate.** This bonding environment is the only one detected at intermediate and high Cu concentration, meaning that it is by far the most abundant. Fig. 8a shows that the EXAFS signal of medium and high Cu NOM yields a considerable similarity with the spectrum of malonate. Unless the macromolecular structure changes with metal loading and influences the first formed metal complex, which is unlikely, this new complex coexists with the five-O-ring chelates formed at lower Cu concentration.

**3.2.2.4. Five-O-ring chelate.** This environment, suggested by the PCA, was identified in the three DOM samples (SPDOM10, SPDOM30, CPDOM30) at low temperature (Fig. 8b). The malate-like 5-O-ring type of spectrum differs in a subtle but systematic and telling way from the malonate-like 6-O-ring spectrum in the  $[5.2\text{--}7.4 \text{ \AA}^{-1}]$  interval (Fig. 9a). In  $\text{Cu}[5\text{-O-ring}]_2$  chelates the maximum amplitude is shifted to higher  $k$  values by  $0.05 \text{ \AA}^{-1}$  relative to  $\text{Cu}[6\text{-O-ring}]_2$  chelates, and the left side of the oscillation contains a strong shoulder in the former, and only a faint hump in the latter. Analysis of CuL and CuL2 carboxylic complexes showed that the absorption shoulder at  $5.8 \text{ \AA}^{-1}$  is characteristic of the 5-O-ring chelate, and is more pronounced,



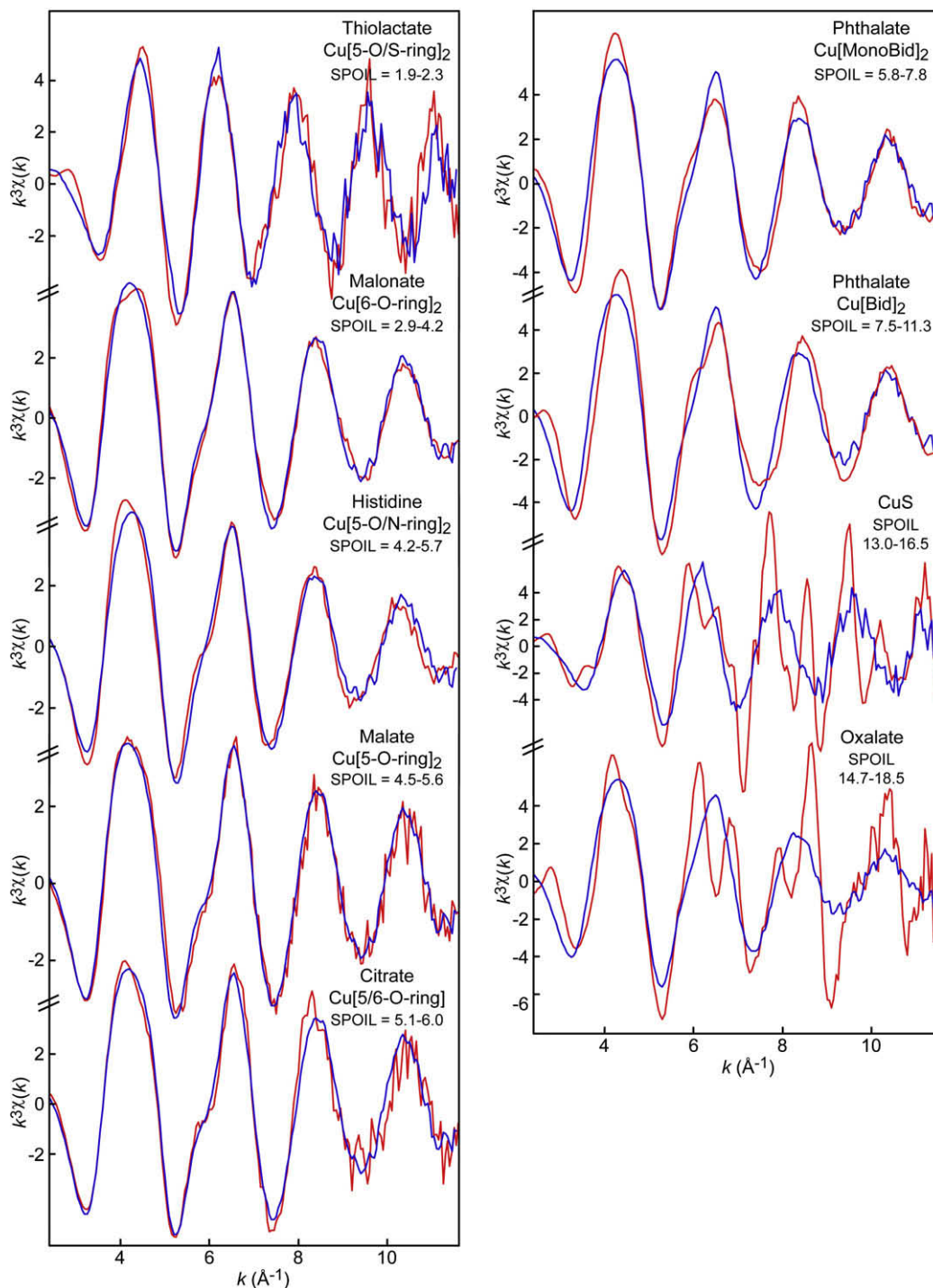


Fig. 7. Target transformations (blue) of the  $k^3\chi(k)$  spectra for model compounds (red). SPOIL values were calculated in the  $[2.0\text{--}11.6 \text{ \AA}^{-1}]$  and  $[2.0\text{--}10.2 \text{ \AA}^{-1}]$  intervals. The citrate reference is a 1:1 complex. The 2:1 complex ( $\text{Cu}(\text{citrate})_2 = \text{Cu}[5/6\text{-O-ring}]_2$ ) has SPOIL values of 6.4 and 8.6. (For interpretation of the references to colours in this figure legend, the reader is referred to the web version of this paper.)

deepening at  $\sim 6.0 \text{ \AA}^{-1}$ , when Cu(II) is bridged to two rings instead of one, as in  $\text{Cu}(\text{citrate})_2$  and  $\text{Cu}(\text{citrate})$  (Fig. 9b–f). This spectral fingerprint was reported previously for mono and bis  $\alpha$ -amino acid chelates (Ozutsumi et al., 1991). Data analysis by Fourier filtering shows that this wave beating results from the interference between SS ( $\text{Cu} \Leftrightarrow \text{O}_{\text{eq}}$  and  $\text{Cu} \Leftrightarrow \text{O}_{\text{ax}}$ ) and MS ( $\text{O}_{\text{eq}} \Leftrightarrow \text{Cu} \Leftrightarrow \text{O}_{\text{eq}}$ ,  $\text{O}_{\text{ax}} \Leftrightarrow \text{Cu} \Leftrightarrow \text{O}_{\text{ax}}$ ,

$\text{Cu} \rightarrow \text{C1} \rightarrow \text{O3}$ ) paths within the 5-O-ring structure (Fig. 9g and h; D'angelo et al., 1998). The SS and MS paths have a near-zero amplitude at  $\sim 5.8 \text{ \AA}^{-1}$  and interfere destructively before and after this value causing a small local beat pattern. In 5-O-ring chelates, the non-bonded O3 atom from the carboxyl group is nearly aligned with the Cu–C1 pair (Cu–C1–O3 angle  $\sim 160^\circ$ ), and thus its scatter-

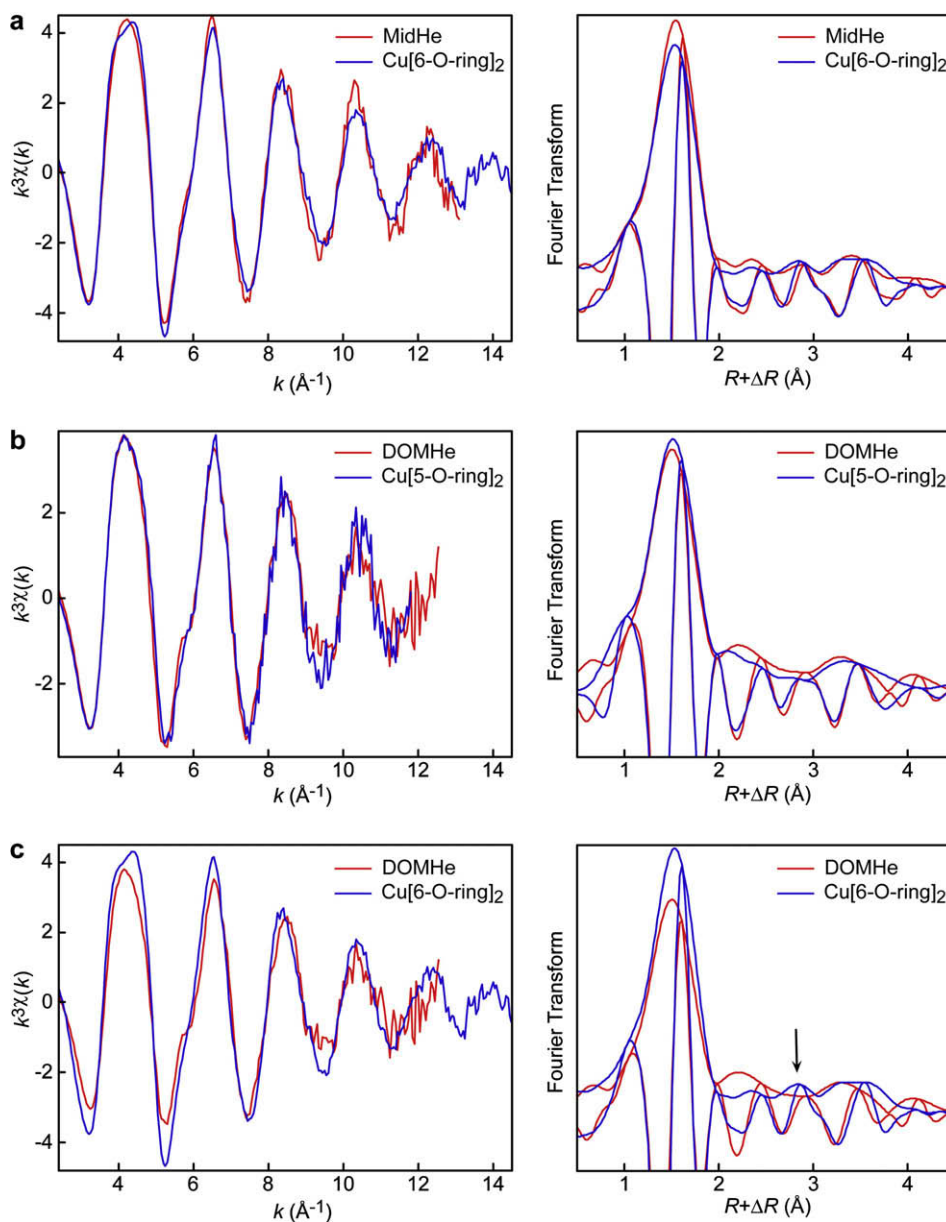


Fig. 8. EXAFS spectra and Fourier transforms for Cu complexed to carboxyl groups at low Cu concentration (DOMHe), and intermediate to high concentration (MidHe), with references. The DOMHe spectrum is the average of SPDOM10, SPDOM30, CPDOM30, and MidHe is the average of CPHA160, CPFA490, SPHA470, SPFA650, and SPFA30. He in the spectrum names stands for liquid helium temperature. With an increase in the Cu concentration, NOM retains most of the Cu[5-O-ring]<sub>2</sub> chelate and begins adding other structures, typically Cu[6-O-ring]<sub>2</sub> chelates.

ing is amplified by a ‘focusing effect’. This path has about the same effective distance as the  $O_{\text{eq}} \Leftrightarrow \text{Cu} \Leftrightarrow O_{\text{eq}}$  path (3.9–4.0 Å), and they both add. The  $O_{\text{ax}} \Leftrightarrow \text{Cu} \Leftrightarrow O_{\text{ax}}$  path is also intense because the two axial oxygens are perpendicular and equidistant from the equatorial plane formed by the two carbon rings. Data simulation showed that the  $O_{\text{ax}}$  atoms are consistently at  $2.32 \pm 0.02$  Å from Cu in DOM and bis-ring chelates, and  $\sim 2.60$  Å from Cu in the bis-bidentate complex (Cu[Bid]<sub>2</sub>).

In reciprocal space, the  $O_{\text{ax}}$  shell at  $\sim 2.32$  Å is phenomenologically reflected by the  $0.05 \text{ \AA}^{-1}$  shift of the maximum

of the second EXAFS oscillation mentioned previously (Fig. 9a). The structure fingerprint of the Cu– $O_{\text{ax}}$  bond at  $\sim 2.32$  Å appears even more clearly when the data are Fourier filtered between  $[1.0\text{--}2.7 \text{ \AA}] R + \Delta R$ , and simulated with the  $O_{\text{eq}}$  and C1 shells, the  $O_{\text{ax}}$  shell being excluded from the fit (Fig. EA2). In real space, the presence of two symmetric Cu– $O_{\text{ax}}$  pairs on both sides of the equatorial plane of DOMHe increases the signal amplitude at  $R + \Delta R = 2.0\text{--}2.2$  Å (SS) and  $\sim 4.0$  Å (MS, Fig. 8c). Also, the C2 peak at  $2.8$  Å  $R + \Delta R$  is absent in the 5-O-ring vs. the 6-O-ring chelate (arrow in Fig. 8c).

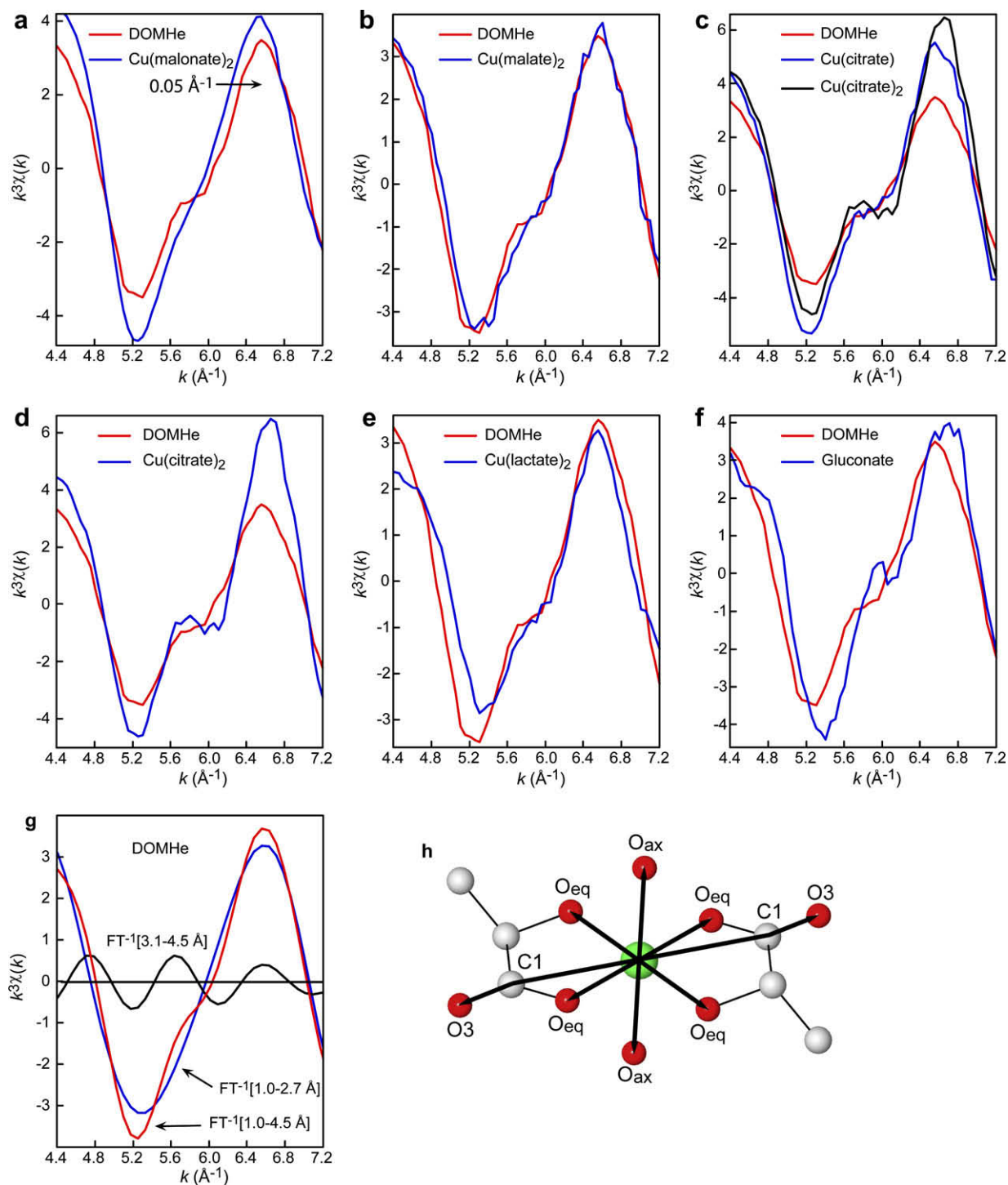


Fig. 9. (a–f) Second oscillation of the EXAFS spectrum for Cu complexed to carboxyl groups at low Cu concentration (DOMHe) with references. This indicator region is sensitive to the size (5-membered vs. 6-membered) and number (mono- vs. bis-chelate) of carbon rings bridged to Cu.  $\text{Cu(citrate)}$  and  $\text{Cu(citrate)}_2$  were recorded in aqueous solution at room temperature,  $\text{Cu(lactate)}_2$  and  $\text{Cu(malate)}_2$  at 10 K in frozen solution, and gluconate as crystalline powder. (g) EXAFS signal for DOMHe filtered in the  $[1.0-2.7 \text{ \AA}]$   $R + \Delta R$  interval (SS paths),  $[3.1-4.5 \text{ \AA}]$  interval (MS paths), and  $[1.0-4.5 \text{ \AA}]$  interval. (h) Schematic representation of the various MS scattering paths (arrowed thick lines).

3.2.2.5. *Five-(O,S)-ring chelate*. Thiolactate-like Cu–NOM bonds were detected at low concentration in four samples: SP10, SP13, SPDOM10\_RT, and SPDOM30\_RT (Fig. 10a). None of these spectra were from pure species.

The two LHe spectra (SP10, SP13) were best fit with a linear combination of  $\sim 1/3$  thiolactate +  $2/3$  malonate (or MidHe), and the two RT spectra with  $\sim 1/2$  thiolactate and  $1/3$  malonate (or MidHe, Fig. 10b,c) Since the

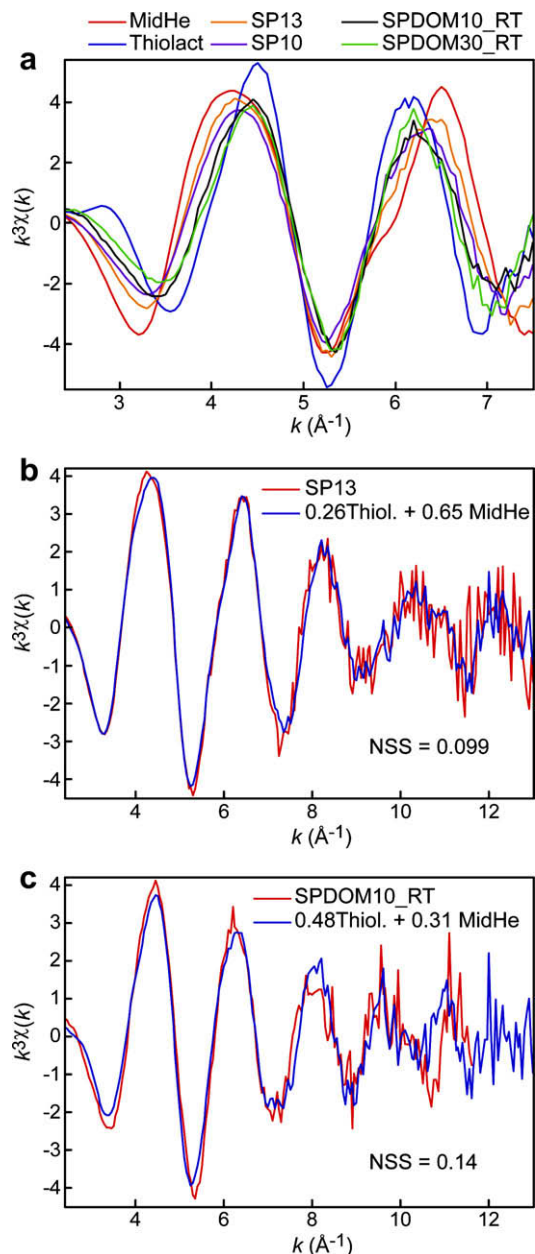


Fig. 10. (a) EXAFS spectra showing the presence of Cu–(O,S) bonds in SP (SP10 and SP13) and their formation at room temperature due to the reduction of Cu(II) to Cu(I) under the X-ray beam (SPDOM10\_RT, SPDOM30\_RT). (b and c) Reconstructions of SP13 and SPDOM10\_RT with linear combinations of MidHe and thiolactate references.

two-component spectra have about the same amplitude, the precision on each species is about 10% total Cu (Isaure et al., 2002; Manceau et al., 2002; Panfili et al., 2005).

## 4. DISCUSSION

### 4.1. Nature of the five- and six-O-ring chelates

Despite the polyfunctional character of NOM and the many possible binding sites and coordination geometries,

all samples can be described with variable proportions of only three key model ligands, all single metal ring chelates: malate, malonate, and thiolactate. There was no hint under our experimental conditions for dimerization of Cu, as observed for some phthalate, benzoate, acetate, and succinate molecular complexes (Koizumi et al., 1963; Cingi et al., 1970, 1977, 1978a,b, 1979; Prout et al., 1971; Brown and Chidambaram, 1973; De Meester et al., 1973; O'Connor and Maslen, 1996; Rodrigues et al., 1999). All experimental data are from mononuclear complexes, in agreement with previous studies of NOM (Davies et al., 1997; Xia et al., 1997; Korshin et al., 1998; Alcacio et al., 2001; Lee et al., 2005; Karlsson and Skjellberg, 2006; Strawn and Baker, 2008). To date, the most elaborate structural model for the binding of Cu to NOM at pH 4.8–6.3 has been proposed by Karlsson and Skjellberg (2006). In this model, Cu(II) is bonded ideally to one 5-(O/N)-ring in soil organic matter and two in DOM, which has molecules with higher flexibility (i.e., lower steric hindrance) because of their lower average molecular weight. The bis-chelate was assumed to be similar to Cu(glutamate)<sub>2</sub>, an amino acid which supposedly coordinates Cu through its amino and carboxyl groups forming a Cu[5-O/N-ring]<sub>2</sub> chelate like Cu(histidine)<sub>2</sub> (Fig. 1). The uniqueness of the glutamate model in the previous study is unknown because its spectrum was not shown, nor was its structure discussed. Instead, Cu(II)-*N*-(phosphonomethyl) glycine (Cu(II)-PMG), a Cu[5/6-O-ring]<sub>2</sub> chelate containing a phosphate ligand, was used as a reference. Our data show that the binding environment of Cu(II) is more like that of  $\alpha$ -OH substituted than  $\alpha$ -NH<sub>2</sub> substituted carboxylates. The ambiguity on the nature of the ring-forming functional group (i.e., Cu[5-O/N-ring]<sub>2</sub> vs. Cu[5/6-O-ring]<sub>2</sub>) can be clarified by examining the structure of the Cu–(glutamate)<sub>2</sub> chelate postulated by Karlsson and Skjellberg (2006) as the best-fit model for NOM. The structure of this chelate was derived by EXAFS (Fitts et al., 1999) from a solution containing a mixture of glutamic acid and copper nitrate at pH 7.5, in which the bis(aminocarboxylato)copper(II)<sub>aq</sub> isomer was assumed to be dominant. Evidence is given below that Cu(II) was likely coordinated to oxygen ligands only, not to oxygen and nitrogen as inferred in Fitts et al. (1999).

The Cu–O<sub>eq</sub> and Cu–N structural distances of Cu–(glutamate)<sub>2aq</sub> are unknown, but in the solid state they are 1.97 and 2.00 Å, respectively (Gramaccioli and Marsh, 1966; Mizutani et al., 1998). These values are typical for Cu(II) binding to amino acid crystals (Table EA1; Orpen et al., 1994), which, for example, are 1.95–1.96 and 1.98–2.02 Å in Cu–(glycine)<sub>2(s)</sub> (Freeman et al., 1964), 1.95 and 2.00 Å in Cu–(aspartate)<sub>(s)</sub> (Calvo et al., 1993), and 1.93–1.99 and 1.98–2.00 Å in Cu–(histidine)<sub>2(s)</sub> (Fig. 1, Evertsson, 1969). On average, the first shell O/N crystallographic distance is 1.98 Å. The same mean value was measured by EXAFS for CuL<sub>2aq</sub>, with L = alanine, serine, threonine, proline, hydroxyproline, and histidine (Ozutsumi et al., 1991). Therefore, the bond distances measured by diffraction on crystals and EXAFS on solutions are close in value, implying that they should be near 1.97 Å for the Cu–O<sub>eq</sub> pair and 2.00 Å for the Cu–N pair in Cu–(glutamate)<sub>2aq</sub>. Distinctive of aminocarboxylates, the Cu–O<sub>eq</sub> crystallographic dis-



tances average out to 1.94 Å in the  $\alpha$ -OH substituted carboxylates salicylate (Hall et al., 1965), malonate (Lenstra and Kataeva, 2001), malate (Zhang, 2007), lactate (Prout et al., 1968), and gluconate (Yodoshi et al., 2006). Consequently, the mean first shell distance is  $1.98 - 1.94 = 0.04$  Å shorter in 5-O-ring (1.94 Å) than in 5-(O/N)-ring (1.98 Å) chelates, thus allowing unambiguous discrimination between the two types of binding environments. However, and unexpectedly, 1.94 Å was also the value measured by EXAFS for Cu–(glutamate)<sub>2aq</sub>, suggesting that Cu was coordinated to OH donors only, and the bis(aminocarboxylato)copper(II) isomer was not the dominant species in the solution studied by Fitts et al. (1999). Therefore, the 1.94 Å Cu–ligand distance determined in this study, and previously by Karlsson and Skyllberg (2006) and earlier investigators (Xia et al., 1997; Korshin et al., 1998; Alcacio et al., 2001; Lee et al., 2005) is more consistent with a chelation by  $\alpha$ -OH substituted carboxylate groups than amino acids. The accuracy of this heuristic value is probably as good as 0.01 Å, because the same Cu–(H<sub>2</sub>O)<sub>aq</sub> bond length (1.97 Å) was used for metrical calibration in the studies by Korshin et al. (1998), Fitts et al. (1999), and Karlsson and Skyllberg (2006).

Karlsson and Skyllberg (2006) determined there were fewer C1 atoms in solid organic matter (SOM) than in DOM, which they interpreted as a decrease of the number of ring chelates from 2 to 1 (i.e., CuL2 to CuL complex). In addition to the loss of C neighbors, the shoulder at  $k = 5.8$  Å<sup>-1</sup> weakened, in agreement with our results. Although reasonable, this interpretation does not account for the existence of the C2 shell at  $R = 3.1$ – $3.2$  Å detected in the present study at LHe temperature in SOM at medium and high Cu concentration. In fact the SOM data are better described with a 6-O-ring model, as shown by the remarkable similarity between the spectra for malonate and SOM (Fig. 8a).

The 5-O-ring and 6-O-ring chelate models agree with infrared and NMR spectroscopy results, which showed that the majority of chelating structures in humics consists of terminal aliphatic carboxyl groups with –OH or –COOH for –H substitution on the carbon in  $\alpha$ -position (Leenheer et al., 1998; Simpson et al., 2001; Strathmann and Myneni, 2004; Deshmukh et al., 2007; Hay and Myneni, 2007). Chelation with an  $\alpha$ -OH yields a 5-membered ring, and chelation with an  $\alpha$ -COOH a 6-membered ring (Fig. 1). Phthalate and salicylate structures, once assumed to be present in large quantities, are now considered less common than previously imagined. At low concentration, they do not seem to be preferred over  $\alpha$ -substituted aliphatic/alicyclic acids as suggested by the higher SPOIL values of the two Cu–phthalate references Cu[Bid]<sub>2</sub> (7.5–11.3) and Cu[MonoBid]<sub>2</sub> (5.8–7.8) (Fig. 7).

#### 4.2. Thermodynamic stability of the O-ring chelates

Thermodynamic formation constants were used to evaluate the relative stabilities of monocarboxylate (lactate, salicylate, furan-2-carboxylate), dicarboxylate (oxalate, malate, malonate, succinate, phthalate) and amino acid (alanine, glutamate) ligands. The relative stabilities of five-,

six-, and seven-O-ring chelates were evaluated with the following isomers:

- The  $\alpha$ -OH isomer of lactic acid, a 5-O-ring C<sub>3</sub> monocarboxylate.
- The  $\beta$ -OH isomer of lactic acid, a 6-O-ring C<sub>3</sub> monocarboxylate.
- The  $\alpha$ -OH isomer of hydroxybutanoic acid, a 5-O-ring C<sub>4</sub> monocarboxylate.
- The  $\beta$ -OH isomer of hydroxybutanoic acid, a 6-O-ring C<sub>4</sub> monocarboxylate.
- The  $\gamma$ -OH isomer of hydroxybutanoic acid, a 7-O-ring C<sub>4</sub> monocarboxylate.

Comparison of equilibrium constants for  $\alpha$ - (2.66),  $\beta$ - (1.82), and  $\gamma$ -OH (1.52) hydroxybutanate, and for  $\alpha$ - (2.59) and  $\beta$ -lactate (1.83, Table 1), shows that the stability of the chelate decreases when the ring size increases, consistent with coordination chemistry concepts (Bell, 1977; Burgess, 1988; Laurie, 1995). Oxalate (4.85) and malonate (5.04) are much stronger complexants than the previous OH substituted organic acids, meaning that a second carboxyl is a better ligand than an hydroxyl. The difference in stability between malonate (dicarboxylate) and lactate (monocarboxylate) can be reduced by adding a second carboxyl in the  $\beta$  position of the  $\alpha$ -OH lactate isomer. This compound is malate (3.63). Thus, Cu–malate is a five-membered chelate, further stabilized by a second carboxyl, as in citrate (3.70, Fig. 1).

Still, speciation calculations with metal stability and proton dissociation constants (i.e., pK<sub>a</sub>) predict that malonate is a better complexant than malate, since 60% of malate and 85% of malonate are predicted to be complexed to Cu(II) at pH 4.5 when [M]/[L] = 0.01. Therefore, the preference of Cu(II) for malate-type over malonate-type structures observed by EXAFS at low concentration in DOM does not follow the trend expected from solution chemistry. This finding agrees with Strathmann and Myneni (2004), who showed using infrared spectroscopy that the stability of Ni chelates follows the order oxalate (strongest) > malate = citrate > malonate > lactate (weakest). Malonate may be over-predicted or malate under-predicted by speciation calculations.

The complexing ability of malate was explained by the formation of a tridentate [5/6-O-ring] chelate with the hydroxyl oxygen and two donor oxygens from the two carboxyls of the same molecule, as in citrate (Strathmann and Myneni, 2004). This coordination is theoretically possible in NOM because carboxyl clusters separated by one alkyl carbon and one alcohol carbon are common structures (Leenheer et al., 1995; Hay and Myneni, 2007). They can be viewed as  $\alpha$ -OH substituted succinate moieties, or a malonate sequence with a COH add-in (HOOC-C-[COH]-COOH). However, this citrate-like model is inconsistent with EXAFS results: the spectra for Cu–malate and Cu–citrate differ significantly, and the C shell in malate and DOM (2.82 and 2.78 Å, Table EA2) is too close for a double (5/6)-O-ring structure (Fig. 4). Thus, EXAFS data are more consistent with a 5-O<sub>eq</sub>-ring structure and two O<sub>ax</sub> atoms linked to carboxyl groups from other chains. For steric reasons,

resulting from the complexity and heterogeneity of NOM, the two Cu–O<sub>ax</sub>–R bonds are likely intermolecular or have carboxyls that are more distant than in the  $\beta$  position. Although citrate-like clusters of COOH groups were identified in NOM, the likelihood of having Cu(II) bonded antisymmetrically to two identical or similar chelates, as in Cu(citrate), seems low.

In general, carboxylate aromatic moieties are weaker chelates because they are unable to form 5-ring malate-type and 6-ring malonate-type structures. Furan-carboxylate, which has only one carboxyl group, is predicted to complex less than 2% Cu at pH 4.5 when  $[M]/[L] = 0.01$ . Thus, Cu(II) is not expected to be bonded to this group at low concentration, despite the relative abundance of O-heterocycles in NOM (Leenheer et al., 1995; Hay and Myneni, 2007). With a  $\beta$ -OH on the C3 carbon, salicylate is analogous to  $\beta$ -OH 3-lactate and 3-hydroxybutanate, and exhibits similar binding strength (5% Cu complexed). Phthalate has two carboxyls, but they are separated by two C atoms (7-O-ring) with no  $\alpha$ -OH substituents, in contrast to malate. Despite the unfavorable size, and also high-strain (see below), of this chelate, phthalate is predicted to complex 30% Cu, for a reason not well understood. The degree of Cu(II) complexation may be over-predicted by speciation calculations, for reasons discussed by Strathmann and Myneni (2004).

Substituting an  $\alpha$ -NH<sub>2</sub> for an  $\alpha$ -OH group increases the thermodynamic stability of Cu(II), as indicated by the five log units increase in  $K$  of the CuL complex from lactate to alanine. Therefore, amino acid-like sites may be as strong as C<sub>3</sub> dicarboxylate clusters. Complexation of Cu(II) to amino acid ligands was suggested in fulvic acids (Senesi and Sposito, 1984; Senesi et al., 1985), and in DOM enriched in proteinaceous material containing 11.9% N (Croué et al., 2003). These chelates were never dominant in our experimental conditions, perhaps because the C to N ratio was too high, or the sorption pH (4.5 and 5.5) was not high enough as suggested by the inferred presence of N ligands using ESR in leaf litter at and above pH 6 (Sposito and Holtzclaw, 1988). Similarly, modeling results from Cu adsorption data presented by Karlsson et al. (2008) suggested that monodentate CuL amino–Cu complex ( $\log K = 9.2$ ) dominated the complexation of Cu over Cu[6-O-ring] chelate ( $\log K = 4.7$ ) in soil peat above pH 6. The bidentate carboxyl complex was dominant at pH 4.5, but the amino complex was again the main species at lower pH, which is improbable. Possible reasons are the omissions in the modeling of the Cu[5-O-ring] chelate, and all CuL<sub>2</sub> complexes. For example, with log stability constants comprised between 14 and 17 (May et al., 1977), CuL<sub>2</sub> amino complexes with a Cu[5-O/N-ring]<sub>2</sub> chelate structure are more likely than CuL amino–Cu complexes at circumneutral pH, as in the xylem sap of plants (Irtelli et al., 2009).

At the beginning of this section, the higher stability of five-membered chelates over higher ring chelates was illustrated with the  $\alpha/\beta/\gamma$ -OH hydroxybutanate isomers and  $\alpha/\beta$ -lactate. This notion can be illustrated also with the Cu[5-O/N-ring]<sub>2</sub> L-histidine chelate. The binding mode of Cu (Fig. 1) shows that the sequence in which the protons

of L-histidine are removed by titration ( $pK_a$ : COOH = 1.8; imidazolium NH = 6.0; NH<sub>3</sub><sup>+</sup> = 9.18) is not the sequence in which the donor atoms are used in copper binding. This is due to the thermodynamic stability of the five-membered COO/NH<sub>2</sub> ring over the six-membered COO/N ring formation involving imidazole group in coordination (Laurie, 1995). If this structural information were not known, adsorption data still could be modeled, but likely with the wrong species because macroscopic measurements lack sensitivity to the actual binding mechanism of the metal. Metal complexes are *abstract* entities (like components in PCA) pre-defined (i.e., arbitrarily chosen) to satisfy mass balance, electric neutrality and proton activity measurements, thus their stabilities and proportions against pH in polyelectrolyte systems depend on the initial hypotheses on their nature. Consequently, there is generally no correspondence between ‘chemical species’ derived from model-dependent titration and adsorption results (Lenoir and Manceau, 2010), and ‘structural species’ derived from spectroscopic and diffraction techniques. Reconciling results from the two approaches is sometimes difficult, as seen previously for the Ni chelates (Strathmann and Myneni, 2004), Cu-phthalate, and the Cu–NOM complexes (Karlsson et al., 2008).

### 4.3. Structural stability of the O-ring chelates

The most stable complex formed between metal ions and polyfunctional molecules occurs where the ionic size matches most closely the size of the binding site or cavity (Hancock, 1989). The strain energy, which is a measure of the size-match fit, is a function of the bond-length and bond-angle deformation, the torsional strain of the chelate, and van der Waals interactions among nonbonded atoms. Divalent Cu has a preference for square (bi)pyramidal coordinations, as a result of its d<sup>9</sup> electronic configuration. By analogy with its coordination chemistry in crown ethers, the torsional strain is minimized when it lies in the plane formed by two ring chelates (Melson, 1979). The strain from bond-length deformation,  $U_B$ , is given by the simple Hooke’s law expression,  $U_B = 1/2K(r^\circ - r)^2$ , where  $r^\circ$  is the ideal bond length,  $r$  is the observed bond length, and  $K$  is the force constant for the particular type of bond (Brubaker and Johnson, 1984). Strain-free (i.e.,  $r = r^\circ$ ) metal-donor lengths generally are derived from crystal structures. The mean Cu(II)–O<sub>eq</sub> distance calculated over 197 structures is  $r^\circ = 1.679 + 0.37\ln(0.5) = 1.94 \text{ \AA}$  (Brown and Altermatt, 1985), the heuristic value for NOM. Malonate represents a low strain energy situation in that the coordination is nearly perfectly square-planar (bond distances of 1.94 and 1.97 Å and O<sub>eq</sub>–Cu–O<sub>eq</sub> angles of 93°), the torsion angles of this chelate  $\pm 13^\circ$ , and the carbon is sp<sup>2</sup> hybridized with O–C–C and C–C–C angles (123°) close in value to benzene (120°) (Fig. 11). The two bonding oxygens are closer in malate (2.57 Å) than in malonate (2.85 Å), since the ring has two instead of three carbons, causing the two O<sub>eq</sub>–Cu–O<sub>eq</sub> angles to decrease from 93° to 83°. The slight departure from the square-planar symmetry is compensated energetically by an increase in ligand field strength through a reduction of the Cu(II)–O<sub>eq</sub> distances from 1.94–1.97 to

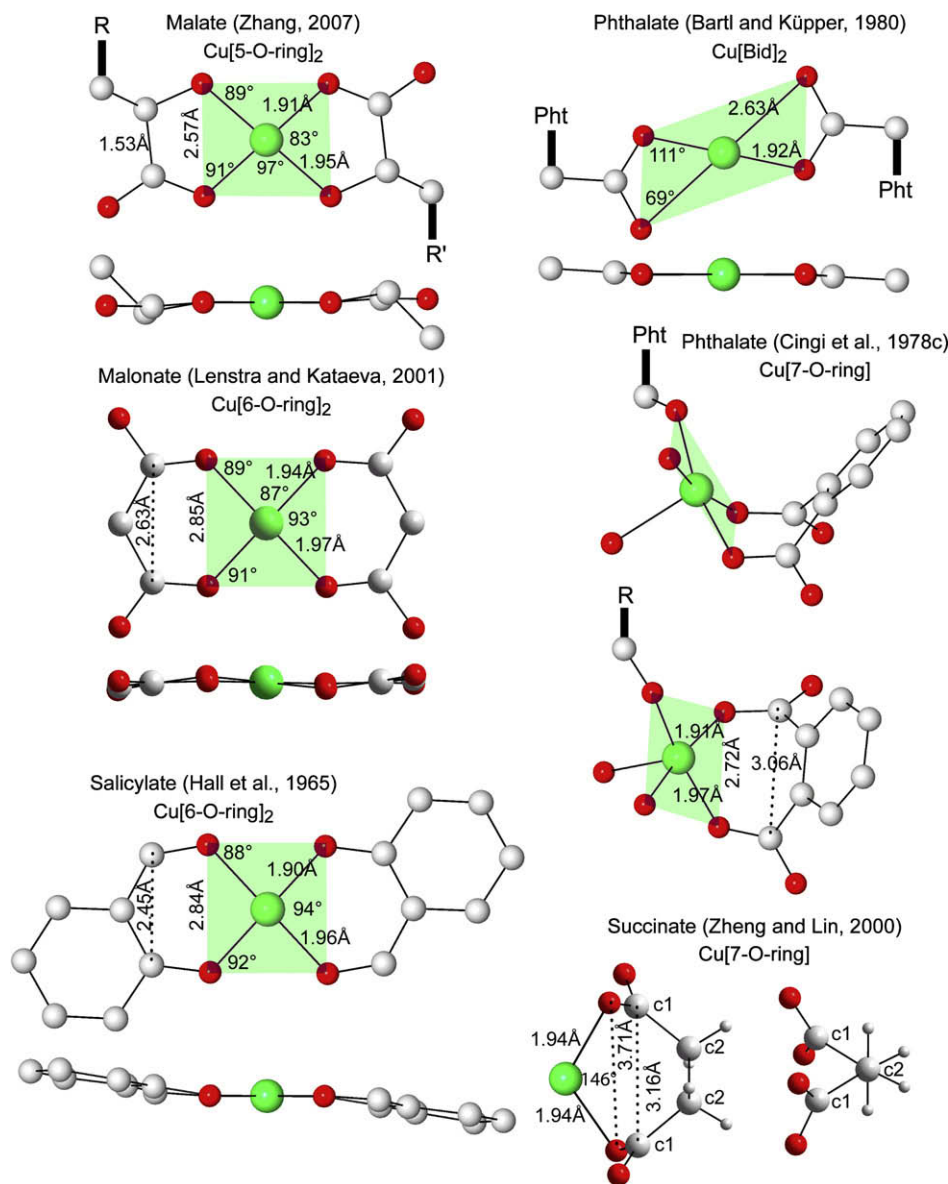


Fig. 11. Top- and lateral-views of the geometry of Cu carboxylate chelates. The O–O distance of 3.71 Å in succinate is unfit for chelation with Cu(II), and in reality Cu forms a bidentate complex (Fig. 4, Table EA1).

1.91–1.95 Å (Boyd et al., 1983). The range of the torsion angles is unchanged ( $-12^\circ$  to  $-10^\circ$ ), and the mean O–C–C bond angle is  $112^\circ$ , a value close to  $109.5^\circ$  for an  $sp^3$  hybridized carbon atom. Thus, the difference in strain energy of Cu–malate and Cu–malonate seems small, but with one hydroxyl ligand close to one carboxyl, and with two carboxyls separated by two carbons as in malonate, malate offers more bonding opportunities.

The low-strain steric requirement is also met in salicylate: the two  $O_{eq}$  are at 1.90 and 1.96 Å from Cu, they are 2.84 Å apart, the  $O_{eq}$ –Cu– $O_{eq}$  angle is  $94^\circ$ , and the torsion angles  $\pm 13^\circ$  (Hall et al., 1965). From a structural standpoint, salicylate ( $\log K = 2.22$ ) should have the same affinity for Cu as malonate ( $\log K = 5.04$ ), since the two molecules have the same 6-O-ring chelate backbone. The

2.8 orders of magnitude difference in their stability constants results from the more electronegative character of carboxyls, making them better ligand donors than alcohol groups. However, when the alcohol group is next to a carboxylate group, like in malate, it acquires more acidic character and becomes more prone to stabilizing the metal complex by acting as a “supporting” donor group in concert with the adjacent carboxylate (Strathmann and Myneni, 2004).

When the open-chain aliphatic ligand contains four carbons and no  $\alpha$ -substituent, as in succinate, the separation between the two nearest carboxyl oxygens is 3.71 Å, too long to accommodate Cu(II) without inducing a strong steric constraint (Fig. 11; Zheng and Lin, 2000). If the molecule were not folded, the  $O_{eq}$ –Cu– $O_{eq}$  angle of the 7-O-ring

chelate would be  $146^\circ$  for  $d(\text{Cu}-\text{O}_{\text{eq}}) = 1.94 \text{ \AA}$ . When a ring chelate has more than three carbons, it is no longer planar, as seen in Fig. 11 with succinate and the phthalate structure determined by Cingi et al. (1978c). The unfavorable 7-O-ring structure of this chelate has the form of a chair, with torsion angles between  $-51^\circ$  and  $61^\circ$ , thus inducing a strong rise in strain energy. When phthalate acts as a bis-bidentate ligand, as in the  $\text{Cu}[\text{Bid}]_2$  reference (Cingi et al., 1969; Bartl and Küppers, 1980), it is also unfit for binding Cu strongly. The coordination about Cu defined by the two planar carboxyl groups is a parallelogram, one O atom from each carboxyl group forming the short diagonal and the second O forming the long diagonal (Fig. 11). The short diagonal is  $2 \times 1.92 = 3.84 \text{ \AA}$  in length, the long diagonal  $2 \times 2.63 = 5.26 \text{ \AA}$ , and the complementary angles are  $69^\circ$  and  $111^\circ$ . In comparison, the four coplanar carboxyl groups from bis-malate bridge Cu nearly in square-planar geometry, thus approaching the favorable  $D_{4h}$  point group tetragonal symmetry.

Therefore, from geometrical considerations, the best-fit size and square (bi)pyramid geometry with four metal–oxygen distances at  $1.94 \text{ \AA}$  are obtained in NOM with  $\alpha$ -OH substituted COOH structures and  $\text{C}_3$  dicarboxylates. Adding one  $\alpha$ -OH group to a  $\text{C}_4$  dicarboxylate, as in citrate, provides more possibilities for complexation. Oxalate-type  $\text{C}_2$  dicarboxylate structures are even stronger chelates, but they are seldom present in NOM.

#### 4.4. The 5-(O,S)-ring chelates

Based on the hard–soft metal classification, Cu(II) is an intermediate metal, and thus may form Cu–S bonds and at the same time coordinate with carboxyls in NOM (Pearson, 1973; Parr and Pearson, 1983; Smith et al., 2002). In addition, the hydroxyl and amine functionalities on the  $\alpha$  carbon are relatively weak Lewis donors, thus a thiolate functionality can anchor Cu(II) balancing the weakness of the Cu(II)–carboxyl bond in forming a 5-(O,S)-ring chelate. In this context, conjugates of thio-carboxylic acids, containing a combination of thiolate and carboxylate functionalities, such as thiolactate and thioacetate, are plausible model ligands. The likelihood of this type of chelate in NOM is supported also by the favorable five-membered arrangements typically observed for bifunctional thiolate-anchored ligands, and the poor reconstruction of the data with CuS (SPOIL = 6.6–8.6).

Overall, cysteinyl sulfur and  $\alpha$ -SH substituted aliphatic carboxylic structures do not seem to play an important role in Cu(II) chelation, in contrast to oxygen donors. Thiolactate-like chelates were detected in SP only, not in its humic, fulvic and DOM fractions, although DOM contains two times more S (Table 2). This increase does not mean that the sample has more reduced sulfur groups because oxidized sulfur is preferentially extracted in hydrophilic water-soluble fractions (Prietzel et al., 2007). However, with 1.1 wt.%

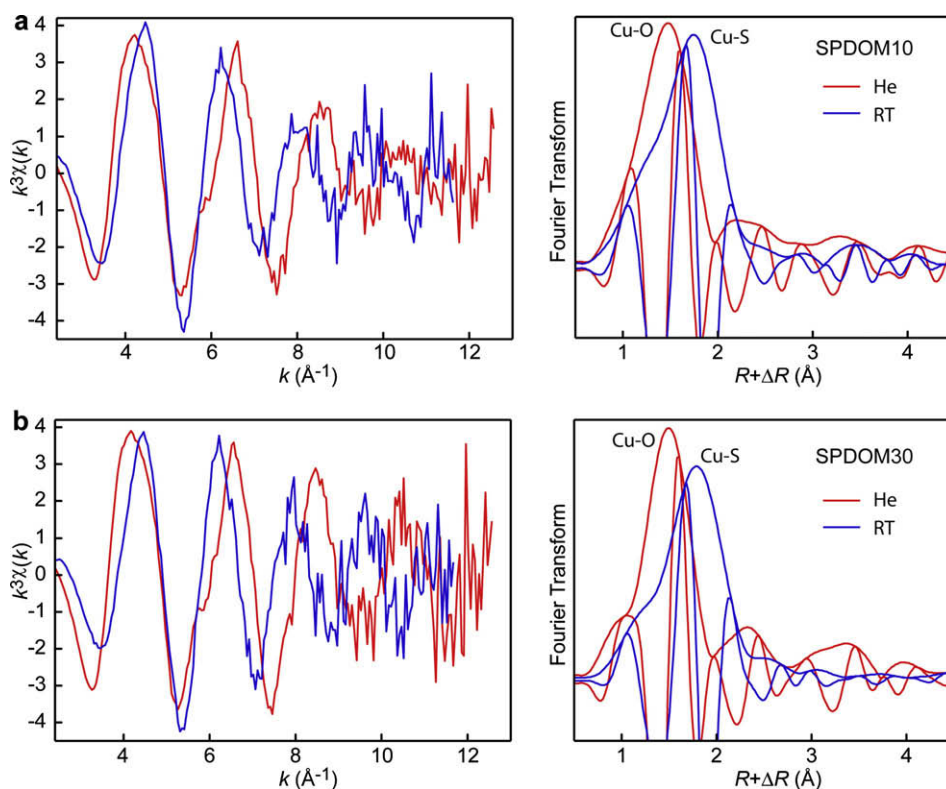


Fig. 12. EXAFS spectra and Fourier transforms of the two DOM samples from the SP peat at room (RT) and liquid helium (He) temperature, showing the formation of Cu–S bonds upon reduction of Cu(II) to Cu(I) by exposure under the beam. The speed at which the X-ray beam reduces divalent Cu is much reduced at low temperature.



S, there should be a large excess of  $S_{\text{red}}$  ligands for SPDOM to bind 100 ppm Cu(II) (sample SPDOM10; Karlsson et al., 2005). Confirming evidence comes from the conversion of Cu(II)–O to Cu(I)–S bonds by radiation damage in the two SPDOM samples (Fig. 12). The formation of strong metal–sulfur bonds following the photoreduction of divalent Cu is consistent with the soft metal character of Cu(I) (Pearson, 1973), and suggests that the hardness of Cu(II) is the main reason for the limited role of –SH ligands in the binding of divalent copper in NOM. The detection by EXAFS of Cd–S bonds in SOM and DOM (Karlsson et al., 2005) also can be explained with the hard and soft metal concept, since Cd(II) is slightly softer than Cu(II). However, in terms of electronegativities metals rank as follows: Au(I) > Ag(I) > Hg(II) ~ Cu(I) > Pb(IV) > Pb(II) > Cu(II) > Cd(II) > Co(II) > Ni(II) > Fe(II) > Mn(II), suggesting that Cu(II) and Cd(II) have similar thiophilicity (Stumm, 1993). These considerations do not take into account the relative stability of the complexes, which depends (among other factors) on the conformation of the chelate, as discussed previously, and the inter- and intra-molecular packing forces and interactions of the metal with other moieties (e.g., hydrogen bonds).

#### 4.5. Affinity of NOM for other metals

The stability constants of divalent metals sorbed to fulvic acid extracted from sewage sludge decrease in the order Pb (4.22) > Cu (3.88) > Ni (3.81) > Zn (3.54) > Cd (3.04) for 1:1 strong complexes with carboxyls (Sposito et al., 1979, 1981). The predicted stability trend of these organo-metal complexes has been confirmed experimentally on NOM from different origins (see e.g., Gao et al., 1997; Vega et al., 2006, and references therein). The stronger binding of Pb(II) with NOM can be explained by its ability to form square pyramidal coordination environments with oxygens, and by its higher softness which conveys a higher affinity for soft donor ligands, such as sulfhydryls, relative to the four other metals. In  $\alpha$ -PbO, the four Pb–O and O–O bond lengths are 2.31 and 2.80 Å, respectively (Leciejewicz, 1961). In  $\beta$ -PbO, the pyramid is distorted with  $R_{\text{Pb-O}} = 2.22$  Å, 2.25 Å,  $2.48 \times 2$  Å and  $R_{\text{O-O}} = 2.94$  Å  $\times 2$  and  $3.03$  Å  $\times 2$  (Hill, 1985). Divalent lead is clearly too big to compete for malate ligands, and more likely forms 6-O-ring chelates with malonate and salicylate ligands (Manceau et al., 1996). Since the coordination of Pb(II) is always pyramidal, as a consequence of the stereoactivity of a 6s2 lone pair of electrons (Wells, 1984; Greenwood and Earnshaw, 1985), Pb is off-centered from the chelate plane, in contrast to Cu(II). A geometry similar to that of Pb(II) has been described recently for Sb(III), which also possesses an outer shell lone pair (5s2 electronic configuration) and strongly sorbs to NOM (Tella and Pokrovski, 2009). However, in this case the preferred chelate structure would be five-membered because Sb(III) is smaller than Pb(II) ( $R_{\text{Sb-O}} = 2.01$ – $2.20$  Å), and the basis of the distorted square pyramid has metrical parameters close to malate ( $R_{\text{O-O}} = 2.65$ – $2.70$  Å; Kamemar et al., 1970). With an [Ar]3d<sup>10</sup> and [Kr]4d<sup>10</sup> electronic configuration, Zn(II) and Cd(II) tend to form regular tetrahedra and octahedra with oxygens, thereby explaining their weaker affinity for NOM.

#### ACKNOWLEDGMENTS

Olivier Proux and Jean Louis Hazemann from the FAME beamline at ESRF, and Matthew Marcus and Sirine Fakra from beamline 10.3.2 at the ALS, are thanked for their assistance during X-ray measurements. We thank Tourbières de France (<http://www.tourbieres.com/>) for providing the peat samples. This manuscript benefited from comments and suggestions by two anonymous reviewers. This research was funded by the EC2CO program from the CNRS, and supported by the Centre National de la Recherche Scientifique (CNRS, France), through the CRG-program at ESRF. The ALS is supported by the Director, Office of Science, Office of Basic Energy Sciences, Materials Sciences Division of the U.S. Department of Energy under Contract DE-AC03-76SF00098 at the Lawrence Berkeley National Laboratory.

#### APPENDIX A. SUPPLEMENTARY DATA

Supplementary data associated with this article can be found, in the online version, at doi:10.1016/j.gca.2010.01.027.

#### REFERENCES

- Alcacio T. E., Hesterberg D., Chou J. W., Martin J. D., Beauchemin S. and Sayers D. E. (2001) Molecular scale characteristics of Cu(II) bonding in goethite–humate complexes. *Geochim. Cosmochim. Acta* **65**, 1355–1366.
- Ankudinov A. L. and Rehr J. J. (1997) Relativistic calculations of spin-dependent X-ray-absorption spectra. *Phys. Rev. B* **56**, 1712–1716.
- Bair R. A. and Goddard W. A. (1980) Ab initio studies of the X-ray absorption edge in copper complexes. I. Atomic Cu<sup>2+</sup> and Cu(II)Cl<sub>2</sub>. *Phys. Rev. B* **22**, 2767–2776.
- Bartl H. and Küppers H. (1980) Neutronenbeugungsuntersuchung der extrem kurzen wasserstoffbrücke in kupfer-dihydrogen-diphthalat-dihydrat. *Z. Kristallogr.* **152**, 161–167.
- Bell C. F. (1977) *Principles and Applications of Metal Chelation*. Clarendon Press.
- Benedetti M. F., van Riemsdijk W. H., Koopal L. K., Kinniburgh D. G., Goody D. C. and Milne C. J. (1996) Metal ion binding by natural organic matter: from the model to the field. *Geochim. Cosmochim. Acta* **60**, 2503–2513.
- Bohlin E., Hämäläinen M. and Sundén T. (1989) Botanical and chemical characterization of peat using multivariate methods. *Soil Sci.* **147**, 252–263.
- Bott R. C., Sagatys D. S., Lynch D. E., Smith G., Kennard C. H. L. and Mak T. C. W. (1991) The preparation and crystal structure of ammonium bis[citrate(3-)]cuprate(II). *Aust. J. Chem.* **44**, 1495–1498.
- Boyd S. A., Sommers L. E. and Nelson D. W. (1981) Copper(II) and iron(III) complexation by the carboxylate group of humic acid. *Soil Sci. Soc. Am. J.* **45**, 1241–1242.
- Boyd S. A., Sommers L. E., Nelson D. W. and West D. X. (1983) Copper(II) binding by humic acid extracted from sewage sludge: an electron spin resonance study. *Soil Sci. Soc. Am. J.* **47**, 43–46.
- Briand G. G., Burford N., Eelman M. D., Aumeerally N., Chen L., Cameron T. S. and Robertson K. N. (2004) Identification, isolation, and characterization of cysteinyl and thiolactate complexes of bismuth. *Inorg. Chem.* **43**, 6495–6500.
- Brown G. M. and Chidambaram R. (1973) Dinuclear copper(II) acetate monohydrate: a redetermination of the structure by neutron-diffraction analysis. *Acta Crystallogr. B* **29**, 2393–2403.

- Brown I. D. and Altermatt D. (1985) Bond-valence parameters obtained from a systematic analysis of the inorganic crystal structure database. *Acta Cryst.* **B41**, 244–247.
- Brubaker G. R. and Johnson D. W. (1984) Molecular mechanics calculations in coordination chemistry. *Coord. Chem. Rev.* **53**, 1–36.
- Burgess J. (1988) *Ions in Solution. Basic Principles of Chemical Interactions*. Ellis Horwood Limited, Chichester, UK.
- Calvo R., Steren C. A., Piro O. E., Rojo T., Zuniga F. J. and Castellano E. E. (1993) Crystal structure and magnetic properties of diaqua(L-aspartato)copper(II). *Inorg. Chem.* **32**, 6016–6022.
- Carrera F., Sanchez Marcos E. S., Merklng P. J., Chaboy J. and Munoz-Paez A. (2004) Nature of metal binding sites in Cu(II) complexes with histidine and related N-coordinating ligands, as studied by EXAFS. *Inorg. Chem.* **43**, 6674–6683.
- Chen X. Y., Shi W., Cheng P., Chen J. T., Yan S. P., Liao D. Z. and Jiang Z. H. (2003) Multi-dimensional copper(II) coordination polymers via self-assembly induced by sodium ions. *Z. Anorg. Allg. Chem.* **629**, 2034–2039.
- Cingi M. B., Guatini C., Musatti A. and Nardelli M. (1969) The crystal and molecular structure of bis(hydrogen *o*-phthalato)diaquocopper(II). *Acta Crystallogr. B* **25**, 1833–1840.
- Cingi M. B., Guastini C., Musatti A. and Nardelli M. (1970) The crystal and molecular structure of diammine-(*o*-phthalato)copper (II). *Acta Crystallogr. B* **26**, 1836–1843.
- Cingi M. B., Lanfredi A. M. M., Camellini A. T. and Camellini M. T. (1977) Influence of the alkaline cation on the structures of polymeric *o*-phthalatoocuprate(II). I. The crystal structures of dilithium catena-di- $\mu$ -(*o*-phthalato)-cuprate(II) tetrahydrate and dirubidium catena-di- $\mu$ -(*o*-phthalato)-cuprate(II) dihydrate. *Acta Crystallogr. B* **33**, 659–664.
- Cingi M. B., Lanfredi A. M. M., Camellini A. T. and Camellini M. T. (1978a) The crystal and molecular structure of *o*-phthalato-copper(II) dihydrate. *Acta Crystallogr. B* **34**, 134–137.
- Cingi M. B., Lanfredi A. M. M., Camellini A. T. and Camellini M. T. (1978b) The crystal and molecular structures of magnesium di-*o*-phthalatocuprate(II) dihydrate and strontium di-*o*-phthalatocuprate(II) trihydrate. *Acta Crystallogr. B* **34**, 406–411.
- Cingi M. B., Lanfredi A. M. M., Tiripicchio A. and Camellini M. T. (1978c) The crystal and molecular structures of barium diaquadi(*o*-phthalato)cuprate(II) dihydrate. An example of the chelating behavior of the *o*-phthalate anion. *Acta Crystallogr. B* **34**, 774–778.
- Cingi M. B., Lanfredi A. M. M., Camellini A. T. and Camellini M. T. (1979) Polymeric chains of tetranuclear hydroxo-*o*-phthalatocuprate(II) units and silver(I)-aromatic interactions in the crystal structure of  $\text{Ag}[\text{Cu}_2(\text{C}_8\text{H}_4\text{O}_4)_2(\text{OH})] \cdot 5\text{H}_2\text{O}$ . *Acta Crystallogr. B* **35**, 312–316.
- Cotton F. A., Wilkinson G., Murillo C. A. and Bochmann M. (1999) *Advanced Inorganic Chemistry*. John Wiley & Sons, New York.
- Covelo E. F., Couce M. L. A. and Vega F. A. (2004) Competitive adsorption and desorption of cadmium, chromium, copper, nickel, lead, and zinc by humic umbrisol. *Commun. Soil Sci. Plant Anal.* **35**, 2709–2729.
- Croué J. P., Benedetti M. F., Violleau D. and Leenheer J. A. (2003) Characterization and copper binding of humic and nonhumic organic matter isolated from the South Platte River: evidence for the presence of nitrogenous binding site. *Environ. Sci. Technol.* **37**, 328–336.
- D'Angelo P., Bottari E., Festa M. R., Nolting H. F. and Pavel N. V. (1998) X-ray absorption study of copper(II)–glycinate complexes in aqueous solution. *J. Phys. Chem. B* **102**, 3114–3122.
- Dance I. G. (1986) The structural chemistry of metal thiolate complexes. *Polyhedron* **5**, 1037–1104.
- Davies G., Fataftah A., Cherkasskiy A., Ghabbour E. A., Radwan A., Jansen S. A., Kolla S., Paciolla M. D., Sein L. T., Buermann W., Balasubramanian M., Budnick J. and Xing B. (1997) Tight metal binding by humic acids and its role in biomineralization. *J. Chem. Soc. Dalton Trans.*, 4047–4060.
- de Meester P., Fletcher S. R. and Skapski A. C. (1973) Refined crystal structure of tetra- $\mu$ -acetato-bisaquodiccoper(II). *J. Chem. Soc. Dalton Trans.*, 2575–2578.
- Deshmukh A. P., Pacheco C., Hay M. B. and Myneni S. C. B. (2007) Structural environments of carboxyl groups in natural organic molecules from terrestrial systems. Part 2. 2D NMR spectroscopy. *Geochim. Cosmochim. Acta* **71**, 3533–3544.
- Dupont L., Guillon E., Bouanda J., Dumonceau J. and Aplincourt M. (2002) EXAFS and XANES studies of retention of copper and lead by a lignocellulosic biomaterial. *Environ. Sci. Technol.* **36**, 5062–5066.
- Evertsson B. (1969) The crystal structure of bis-L-histidine-copper(II) dinitrate dihydrate. *Acta Crystallogr. B* **25**, 30–41.
- Fitts J. P., Persson P., Brown G. E. J. and Parks G. E. (1999) Structure and bonding of Cu(II)–glutamate complexes at the  $\gamma$ - $\text{Al}_2\text{O}_3$ –water interface. *J. Colloid Interf. Sci.* **320**, 133–147.
- Freeman H. C., Snow M. R., Nitta I. and Tomita K. (1964) A refinement of the structure of bisglycinocopper(II) monohydrate,  $\text{Cu}(\text{NH}_2\text{CH}_2\text{COO})_2 \cdot \text{H}_2\text{O}$ . *Acta Crystallogr.* **17**, 1463–1470.
- Frenkel A. I., Korshin G. V. and Ankudinov A. L. (2000) XANES study of  $\text{Cu}^{2+}$ -binding sites in aquatic humic substances. *Environ. Sci. Technol.* **34**, 2138–2142.
- Gao S. A., Walker W. J., Dahlgren R. A. and Bold J. (1997) Simultaneous sorption of Cd, Cu, Ni, Zn, Pb, and Cr on soils treated with sewage sludge supernatant. *Water Air Soil Pollut.* **93**, 331–345.
- Gazo J., Bersuker I. B., Garaj J., Kabesova M., Kohot J., Langfelderova H., Melnik M., Serator M. and Valach F. (1976) Plasticity of coordination sphere of copper(II) complexes. Its manifestation and causes. *Coord. Chem. Rev.* **19**, 253–297.
- Goeta A. E., Rigotti G., Sileo E. E. and Blesa M. A. (1993) Structure and reactivity of copper(II) carboxylates II. Copper(II) bis(hydrogen *o*-phthalate)dihydrate. *Solid State Ionics* **62**, 159–165.
- Gramaccioli C. M. and Marsh R. E. (1966) The crystal structure of copper glutamate dihydrate. *Acta Crystallogr.* **21**, 594–600.
- Greenwood N. N. and Earnshaw A. (1985) *Chemistry of the Elements*. Pergamon Press.
- Gregor J. E., Powell H. K. J. and Town R. M. (1989a) Evidence for aliphatic mixed-mode coordination in copper(II)–fulvic acid complexes. *J. Soil Sci.* **40**, 661–673.
- Gregor J. E., Powell H. K. J. and Town R. M. (1989b) Metal–fulvic acid complexing: evidence supporting an aliphatic carboxylate mode of coordination. *Sci. Total Environ.* **81**, 597–606.
- Grunes L. A. (1983) Study of the K edges of 3D transition-metals in pure and oxide form by X-ray absorption spectroscopy. *Phys. Rev. B* **27**, 2111–2131.
- Hahn J. E., Scott R. A., Hodgson K. O., Doniach D., Dejardins S. E. and Solomon E. I. (1982) Observation of an electric quadrupole transition in the X-ray absorption spectrum of a Cu(II) complex. *Chem. Phys. Lett.* **88**, 595–598.
- Hall D., McKinnon A. J. and Waters T. N. (1965) The colour isomerism and structure of copper coordination compounds. Part VIII. The crystal structure of a second crystalline form of bis-salicylaldehydatocopper(II). *J. Chem. Soc.*, 425–430.
- Hancock R. D. (1989) Ligand design for selective complexation of metal ion in aqueous solution. *Chem. Rev.* **89**, 1875–1914.
- Hay M. B. and Myneni S. C. B. (2007) Structural environments of carboxyl groups in natural organic molecules from terrestrial

- systems. Part 1. Infrared spectroscopy. *Geochim. Cosmochim. Acta* **71**, 3518–3532.
- Hering J. G. and Morel F. M. M. (1988) Humic-acid complexation of calcium and copper. *Environ. Sci. Technol.* **22**, 1234–1237.
- Hill R. J. (1985) Refinement of the structure of orthorhombic PbO (massicot) by Rietveld analysis of neutron powder diffraction data. *Acta Crystallogr. C* **41**, 1281–1284.
- Irtelli B., Petrucci W. A. and Navari-Izzo F. (2009) Nicotianamine and histidine/proline are, respectively, the most important copper chelators in xylem sap of *Brassica carinata* under conditions of copper deficiency and excess. *J. Exp. Bot.* **60**, 269–277.
- Isaure M. P., Laboudigue A., Manceau A., Sarret G., Tiffreau C., Trocellier P., Hazemann J. L. and Chateigner D. (2002) Quantitative Zn speciation in a contaminated dredged sediment by  $\mu$ PIXE,  $\mu$ SXRF, EXAFS spectroscopy and principal component analysis. *Geochim. Cosmochim. Acta* **66**, 1549–1567.
- Kamenar B., Grdenic D. and Prout C. K. (1970) The crystal and molecular structure of racemic potassium di- $\mu$ -tartrato-dian-timonate(III) trihydrate (racemic ‘tartar emetic’). *Acta Crystallogr. B* **26**, 181–188.
- Karlsson T., Persson P. and Skyllberg U. (2005) Extended X-ray absorption fine structure spectroscopy evidence for the complexation of cadmium by reduced sulfur groups in natural organic matter. *Environ. Sci. Technol.* **39**, 3048–3055.
- Karlsson T. and Skyllberg U. (2006) Complexation of copper(II) in organic soils and in dissolved organic matter – EXAFS evidence for chelate ring structures. *Environ. Sci. Technol.* **40**, 2623–2628.
- Karlsson T., Elgh-Dalgren K. and Skyllberg U. (2008) Modeling copper(II) complexation in a peat soil based on spectroscopic structural information. *Soil Sci. Soc. Am. J.* **72**, 1286–1291.
- Kau L. S., Spira-Solomon D. J., Penner-Hahn J. E., Hodgson K. O. and Solomon E. I. (1987) X-ray absorption edge determination of the oxidation state and coordination number of copper: application to the type 3 site in *Rhus vernicifera* Laccase and its reaction with oxygen. *J. Am. Chem. Soc.* **109**, 6433–6442.
- Kinniburgh D. G., van Riemsdijk W. H., Koopal L. K., Borkovec M., Benedetti M. F. and Avena M. J. (1999) Ion binding to natural organic matter: competition, heterogeneity, stoichiometry and thermodynamic consistency. *Colloid Surf. A Phys. Eng. Aspects* **151**, 147–166.
- Kirpichtchikova T., Manceau A., Spadini L., Panfili F., Marcus M. A. and Jacquet T. (2006) Speciation and solubility of heavy metals in contaminated soil using X-ray microfluorescence, EXAFS spectroscopy, chemical extraction, and thermodynamic modelling. *Geochim. Cosmochim. Acta* **70**, 2163–2190.
- Kogut M. B. and Voelker B. M. (2001) Strong copper-binding behavior of terrestrial humic substances in seawater. *Environ. Sci. Technol.* **35**, 1149–1156.
- Koizumi H., Osaki K. and Watanabe T. (1963) Crystal structure of cupric benzoate trihydrate  $\text{Cu}(\text{C}_6\text{H}_5\text{COO})_2 \cdot 3\text{H}_2\text{O}$ . *J. Phys. Soc. Jpn.* **18**, 117–124.
- Korshin G. V., Frenkel A. I. and Stern E. A. (1998) EXAFS study of the inner shell structure in copper(II) complexes with humic substances. *Environ. Sci. Technol.* **32**, 2699–2705.
- Kosugi N., Yokoyama T., Asakura K. and Kuroda H. (1984) Polarized Cu K-edge XANES of square planar  $\text{CuCl}_4^{2-}$  ion. Experimental and theoretical evidence for shake-down phenomena. *Chem. Phys.* **91**, 249–256.
- Laurie S. H. (1995) *Handbook of Metal-Ligand Interactions in Biological Fluids – Bioinorganic Chemistry*, vol. 2. Marcel Dekker, New York, p. 603.
- Leciejewicz J. (1961) On the crystal structure of tetragonal (red) PbO. *Acta Crystallogr.* **14**, 1304–1305.
- Lee Y. J., Elzinga E. J. and Reeder R. J. (2005) Cu(II) adsorption at the calcite–water interface in the presence of natural organic matter: kinetic studies and molecular-scale characterization. *Geochim. Cosmochim. Acta* **69**, 49–61.
- Leenheer J. A., Brown G. K., MacCarthy P. and Cabaniss S. E. (1998) Models of metal binding structures in fulvic acid from the Suwannee River, Georgia. *Environ. Sci. Technol.* **32**, 2410–2416.
- Leenheer J. A., Wershaw R. L. and Reddy M. M. (1995) Strong-acid, carboxyl-group structures in fulvic acid from the Suwannee river, Georgia. 2. Major structures. *Environ. Sci. Technol.* **29**, 399–405.
- Lenoir T. and Manceau A. (2010) Number of independent parameters in the potentiometric titration of humic substances. *Langmuir*. doi:10.1021/la9034084.
- Lenstra A. T. H. and Kataeva O. N. (2001) Structures of copper(II) and manganese(II) di(hydrogen malonate) dihydrate; effects of intensity profile truncation and background modelling on structure models. *Acta Crystallogr. B* **57**, 497–506.
- Luster J., Lloyd T. and Sposito G. (1996) Multi-wavelength molecular fluorescence spectrometry for quantitative characterization of copper(II) and aluminum(III) complexation by dissolved organic matter. *Environ. Sci. Technol.* **30**, 1565–1574.
- Malinowski E. R. (1977) Determination of the number of factors and the experimental error in a data matrix. *Anal. Chem.* **49**, 612–617.
- Malinowski E. R. (1978) Theory of error for target factor analysis with applications to mass spectrometry and nuclear magnetic resonance spectrometry. *Anal. Chim. Acta* **103**, 354–359.
- Malinowski E. R. (1991) *Factor Analysis in Chemistry*. John Wiley, New York.
- Manceau A., Boisset M. C., Sarret G., Hazemann J. L., Mench M., Cambier P. and Prost R. (1996) Direct determination of lead speciation in contaminated soils by EXAFS spectroscopy. *Environ. Sci. Technol.* **30**, 1540–1552.
- Manceau A., Marcus M. A. and Tamura N. (2002) Quantitative speciation of heavy metals in soils and sediments by synchrotron X-ray techniques. In *Applications of Synchrotron Radiation in Low-temperature Geochemistry and Environmental Science*, vol. 49 (eds. P. A. Fenter, M. L. Rivers, N. C. Sturchio and S. R. Sutton). Mineralogical Society of America, Washington, DC.
- Marcus M. A., MacDowell A. A., Celestre R., Manceau A., Miller T., Padmore H. A. and Sublett R. E. (2004) Beamline 10.3.2 at ALS: a hard X-ray microprobe for environmental and materials sciences. *J. Synchrotron Radiat.* **11**, 239–247.
- Mathur S. P. and Farnham S. R. (1985) Geochemistry of humic substances in natural and cultivated petlands. In *Humic Substances in Soil Sediment and Water. Geochemistry, Isolation and Characterization* (eds. G. R. Aiken, D. M. McKnight, R. L. Wershaw and P. MacCarthy). Wiley-Interscience, New York, pp. 53–85.
- Matynia A. (2009) Mécanisme de rétention du cuivre sur de la tourbe végétalisée. Ph. D. Thesis, University Joseph Fourier, Grenoble, France.
- May P. M., Linder P. W. and Williams D. R. (1977) Computer simulation of metal-ion equilibria in biofluids: models for the low-molecular-weight complex distribution of calcium(II), magnesium(II), manganese(II), iron(III), copper(II), zinc(II) and lead(II) ions in human blood plasma. *J. Chem. Soc.* **13**, 588–595.
- McBride M. B., Sauve S. and Hendershot W. (1997) Solubility control of Cu, Zn, Cd, and Pb in contaminated soils. *Eur. J. Soil Sci.* **48**, 337–346.

- McLaren R. G., Williams J. G. and Swift R. S. (1983) Some observations on the desorption and distribution behaviour of copper with soil components. *J. Soil Sci.* **34**, 325–331.
- Melnik M., Kabesova M., Koman M., Macaskova L., Garaj J., Holloway C. E. and Valent A. (1998a) Copper(II) coordination compounds: classification and analysis of crystallographic and structural data. III. Dimeric compounds. *J. Coord. Chem.* **45**, 147–359.
- Melnik M., Kabesova M., Macaskova L. and Holloway C. E. (1998b) Copper(II) coordination compounds: classification and analysis of crystallographic and structural data. II. Mononuclear-, hexa-, hepta- and octa-coordinate compounds. *J. Coord. Chem.* **45**, 31–145.
- Melnik M., Kabesova M., Koman M., Macaskova L. and Holloway C. E. (1999) Copper(II) coordination compounds: classification and analysis of crystallographic and structural data. IV. Trimeric and oligomeric compounds. *J. Coord. Chem.* **48**, 271–374.
- Melson G. A. (1979) *Coordination Chemistry of Macrocyclic Compounds*. Plenum Press, New York.
- Mesu J. G., Beale A. M., de Groot F. M. F. and Weckhuysen B. M. (2006) Probing the influence of X-rays on aqueous copper solutions using time-resolved in situ combined video/X-ray absorption near-edge/ultraviolet–visible spectroscopy. *J. Phys. Chem. B* **110**, 17671–17677.
- Mizutani M., Maejima N., Jitsukawa K., Masuda H. and Einaga H. (1998) An infinite chiral single-helical structure formed in Cu(II)-L-/D-glutamic acid system. *Inorg. Chim. Acta* **283**, 105–110.
- O'Connor B. H. and Maslen E. N. (1996) The crystal structure of Cu(II) succinate dihydrate. *Acta Crystallogr.* **20**, 824–835.
- Ogawa T., Shimoï M. and Ouchi A. (1982) Structure and properties of diaquabis(ethylthioacetato)copper(II),  $[\text{Cu}(\text{C}_4\text{H}_7\text{SO}_2)_2(\text{H}_2\text{O})_2]$ . *Bull. Chem. Soc. Jpn.* **55**, 126–129.
- Orpen A. G., Brammer L., Allen F. K., Kennard O., Watson D. G. and Taylor R. (1994) *Structure Correlation, vol. 2*. VCH, New York.
- Ozutsumi K., Miyata Y. and Kawashima T. (1991) EXAFS and spectrophotometric studies on the structure of mono- and bis(aminocarboxylato)copper (II) complexes in aqueous solution. *J. Inorg. Biochem.* **44**, 97–108.
- Panfili F., Manceau A., Sarret G., Spadini L., Kirpichtchikova T., Bert V., Laboudigue A., Marcus M. A., Ahamdach N. and Libert M. F. (2005) The effect of phytostabilization on Zn speciation in a dredged contaminated sediment using scanning electron microscopy, X-ray fluorescence, EXAFS spectroscopy and principal components analysis. *Geochim. Cosmochim. Acta* **69**, 2265–2284.
- Parr R. G. and Pearson R. G. (1983) Absolute hardness – companion parameter to absolute electronegativity. *J. Am. Chem. Soc.* **105**, 7512–7516.
- Pearson R. G. (1973) *Hard and Soft Acids and Bases*. Dowden Hutchinson and Ross Inc., Stroudsburg, PA.
- Powers L. (1982) X-ray absorption spectroscopy. Application to biological molecules. *Biochim. Biophys. Acta* **638**, 1–38.
- Prietzl J., Thieme J., Salome M. and Knicker H. (2007) Sulfur K-edge XANES spectroscopy reveals differences in sulfur speciation of bulk soils, humic acid, fulvic acid, and particle size separates. *Soil Biol. Biochem.* **39**, 877–890.
- Prout C. K., Armstrong R. A., Carruthers J. R., Forrest J. G., Murray-Rust P. and Rossotti F. J. C. (1968) Structure and stability of carboxylate complexes. Part I. The crystal and molecular structures of copper(II) glycolate, DL-lactate, 2-hydroxy-2-methylpropionate, methoxyacetate, and phenoxyacetate. *J. Am. Chem. Soc.*, 2791–2813.
- Prout C. K., Carruthers J. R. and Rossotti F. J. C. (1971) Structure and stability of carboxylate complexes. Part IX. Crystal and molecular structure of copper(II) phthalate monohydrate. *J. Chem. Soc. A*, 3350–3354.
- Proux O., Nassif V., Prat A., Ulrich O., Lahera E., Biquard X., Menthonnex J. J. and Hazemann J. L. (2006) Feedback system of a liquid-nitrogen-cooled double-crystal monochromator: design and performances. *J. Synchrotron Radiat.* **13**, 59–68.
- Ramos L., Hernandez L. M. and Gonzalez M. J. (1994) Sequential fractionation of copper, lead, cadmium and zinc in soils from or near Donana National Park. *J. Environ. Qual.* **23**, 50–57.
- Ressler T. (1998) WinXAS: a program for X-ray absorption spectroscopy data analysis under MS-Windows. *J. Synchrotron Radiat.* **5**, 118–122.
- Ressler T., Wong J., Roos J. and Smith I. (2000) Quantitative speciation of Mn-bearing particulates emitted from autos burning (methylcyclopentadienyl)manganese tricarbonyl-added gasolines using XANES spectroscopy. *Environ. Sci. Technol.* **34**, 950–958.
- Ringqvist L. and Oborn I. (2002) Copper and zinc adsorption onto poorly humified *Sphagnum* and *Carex* peat. *Water Res.* **36**, 2233–2242.
- Rodrigues B. L., Costa M. D. D. and Fernandes N. G. (1999) Diaquabis(hydrogen phthalato)copper(II), a new phase. *Acta Crystallogr. C* **55**, 1997–2000.
- Santos-Echeandia J., Laglera L., Prego R. and van den Berg C. (2008) Copper speciation in continental inputs to the Vigo Ria: sewage discharges versus river fluxes. *Mar. Pollut. Bull.* **56**, 308–317.
- Sarret G., Balesdent J., Bouziri L., Garnier J. M., Marcus M. A., Geoffroy N., Panfili F. and Manceau A. (2004) Zn speciation in the organic horizon of a contaminated soil by micro X-ray fluorescence, micro and powder EXAFS spectroscopy and isotopic dilution. *Environ. Sci. Technol.* **38**, 2792–2801.
- Senesi N., Bocian D. F. and Sposito G. (1985) Electron spin resonance investigation of copper(II) complexation by soil fulvic acid. *Soil Sci. Soc. Am. J.* **49**, 114–119.
- Senesi N. and Sposito G. (1984) Residual copper(II) complexes in purified soil and sewage sludge fulvic acids: electron spin resonance study. *Soil Sci. Soc. Am. J.* **48**, 1247–1253.
- Simpson A. J., Burdon J., Graham C. L., Hayes M. H. B., Spencer N. and Kingery W. L. (2001) Interpretation of heteronuclear and multidimensional NMR spectroscopy of humic substances. *Eur. J. Soil Sci.* **52**, 495–509.
- Smith D. S., Bella R. A. and Kramer B. J. R. (2002) Metal speciation in natural waters with emphasis on reduced sulfur groups as strong metal binding sites. *Comp. Biochem. Physiol. C* **133**, 65–74.
- Smith S. M. and Martell A. E. (2004) Critically selected stability constants of metal complexes database. Standard reference database 46, version 8.0, NIST, Gaithersburg.
- Sposito G. and Holtzclaw K. M. (1988) Fluorescence quenching and copper complexation by a chestnut leaf litter extract: spectroscopic evidence. *Soil Sci. Soc. Am. J.* **52**, 632–636.
- Sposito G., Holtzclaw K. M. and LeVesque-Madore C. S. (1979) Cupric ion complexation by fulvic acid extracted from sewage sludge–soil mixtures. *Soil Sci. Soc. Am. J.* **43**, 1148–1155.
- Sposito G., Holtzclaw K. M. and LeVesque-Madore C. S. (1981) Trace-metal complexation by fulvic acid extracted from sewage-sludge. 1. Determination of stability constants and linear correlation analysis. *Soil Sci. Soc. Am. J.* **45**, 465–468.
- Strathmann T. J. and Myneni S. C. B. (2004) Speciation of aqueous Ni(II)–carboxylate and Ni(II)–fulvic acid solutions: combined ATR–FTIR and XAFS analysis. *Geochim. Cosmochim. Acta* **68**, 3441–3458.



- Strawn D. and Baker L. L. (2008) Speciation of Cu in a contaminated agricultural soil measured by XAFS,  $\mu$ -XAFS, and  $\mu$ -XRF. *Environ. Sci. Technol.* **42**, 37–42.
- Stumm W. (1993) *Chemistry of the Solid–Water Interface*. John Wiley & Sons, New York.
- Swift R. S. (1996) *Organic Matter Characterization*. Soil Science Society of America and American Society of Agronomy, Madison.
- Tan K. H. (2003) *Humic Matter in Soil and the Environment*. Marcel Dekker, New York.
- Tella M. and Pokrovski G. S. (2009) Antimony(III) complexing with O-bearing organic ligands in aqueous solution: an X-ray absorption fine structure spectroscopy and solubility study. *Geochim. Cosmochim. Acta* **73**, 268–290.
- Town R. M. and Powell H. K. J. (1993) Ion-selective electrode potentiometric studies on the complexation of copper(II) by soil-derived humic and fulvic-acids. *Anal. Chim. Acta* **279**, 221–233.
- Vega F. A., Covelo E. F. and Andrade M. L. (2006) Competitive sorption and desorption of heavy metals in mine soils: influence of mine soil characteristics. *J. Colloid Interf. Sci.* **298**, 582–592.
- Wang X. Y., Deng X. T. and Wang C. G. (2006) Bis(acetato- $\kappa^2O,O'$ )diaquacopper(II). *Acta Crystallogr. E* **62**, 3573–3579.
- Wasserman S. R., Allen P. G., Shuh D. K., Bucher J. J. and Edelstein N. M. (1999) EXAFS and principal component analysis: a new shell game. *J. Synchrotron Radiat.* **6**, 284–286.
- Wells A. F. (1984) *Structural Inorganic Chemistry*. Oxford University Press.
- Wright J. G., Natan M. J., McDonnell F. M., Ralston D. M. and O'Halloran T. V. (1990) In *Prog. Inorg. Chem.*, vol. 38 (ed. S. J. Lippart). John Wiley and Sons, New York.
- Xia K., Bleam W. and Helmke P. A. (1997) Studies of the nature of  $\text{Cu}^{2+}$  and  $\text{Pb}^{2+}$  binding sites in soil humic substances using X-ray absorption spectroscopy. *Geochim. Cosmochim. Acta* **61**, 2211–2221.
- Yodoshi M., Odoko M. and Okabe N. (2006) Aqua(di-2-pyridylamine- $\kappa^2N^2,N^2$ )(D-gluconato- $\kappa^2O,O'$ )copper(II) trihydrate. *Acta Crystallogr. E* **62**, 2021–2023.
- Zhang X. Y. (2007) Diaquabis(malato- $\kappa^2O^1,O^2$ )copper(II). *Acta Crystallogr. E* **63**, m1254–m1255.
- Zheng Y. Q. and Lin J. L. (2000) Crystal structure of disodium disuccinatocuperate octahydrate,  $\text{Na}_2\text{Cu}(\text{C}_4\text{H}_4\text{O}_4)_2 \cdot \text{H}_2\text{O}$ . *Z. Kristallogr.* **215**, 165–166.

Associate editor: Donald L. Sparks